DESIGN METHODOLOGY FOR PERMEABLE REACTIVE BARRIERS COMBINED WITH MONITORED NATURAL ATTENUATION

Hafsi Amine

Thesis submitted to the faculty of the
Virginia Polytechnic Institute and State University
In partial fulfillment of the requirements for the degree of

Master of Science
in
Civil Engineering

Dr. George M. Filz, Committee Member

Dr. John C. Little, Committee Member

Dr. Mark A. Widdowson, Chairman

April 23, 2008
Blacksburg, Virginia

Design Methodology for Permeable Reactive Barriers Combined with Monitored Natural Attenuation

Amine Hafsi

The Charles E. Via Department of Civil Engineering

(ABSTRACT)

Permeable reactive barrier (PRB) technology is increasingly considered for in situ treatment of contaminated groundwater; however, current design formulas for PRBs are limited and do not properly account for all major physical and attenuation processes driving remediation. This study focused on developing a simple methodology to design PRBs that is easy to implement while improving accuracy and being more conservative than the available design methodologies. An empirical design equation and a simple analytical design equation were obtained to calculate the thickness of a PRB capable of degrading a contaminant from a source contaminant concentration C_s to a maximum contaminant level C_{MCL} at a Point of compliance POC. Both equations integrate the fundamental components that drive the natural attenuation process of the aquifer and the reactive capacity of the PRB. The empirical design equation was derived from a dataset of random hypothetical cases that used the solutions of the PRB conceptual model (Solution I). The analytical design equation was derived from particular solutions of the model (Solution II) which the study showed fit the complex solutions of the model well. Using the hypothetical cases, the analytical equation has shown that it gives an estimated thickness of the PRB just 15 % lower or higher than the real thickness of the PRB 95 percent of the time. To calculate the design thickness of a PRB, Natural attenuation capacity of the aquifer can be estimated from the observed contaminant concentration changes along aquifer flowpaths prior to the installation of a PRB. Bench-scale or pilot testing can provide good estimates of the required residence times (Gavaskar et al. 2000), which will provide the reactive capacity of the PRB needed for the calculation. The results of this study suggest also that the installation location downgradient from the source of contaminant is flexible. If a PRB is installed in two different locations, it will achieve the same remediation goals. This important finding gives engineers and scientists the choice to adjust the location of their PRBs so that the overall project can be the most feasible and cost effective.

ACKNOWLEDGMENTS

I would like to acknowledge my advisor, Dr. Mark Widdowson, for his support and guidance throughout my studies as a master's student and thank him for the opportunity to contribute towards the understanding of this research. Our many conversations helped in guiding this research to the right direction.

I would like to give a special thank you to my wife, Jeanie, for her patience, help and support. Thanks for sticking with me through all the ups and downs on this journey. Without you, I would have never graduated.

To my daughter Jennah Aida, who reminds me everyday why it is important to work hard and achieve my goals.

To my parents, Mohamed and Fethia, my brother and sister, thanks for all your love and support.

TABLE OF CONTENTS

CHAPTER 1 1

INTRODUCTION 1

1.1 Background *1*

1.2 Natural Attenuation *3*

1.3 Zero-Valent Iron *4*

1.4 Permeable Reactive Barriers *5*

1.5 Existing Design Methodologies for PRBs *10*

REFERENCES 12

CHAPTER 2 ..... **15**

MATHEMATICAL MODEL AND SOLUTIONS 15

2.1 Objective *15*

2.2 Governing Equations *16*

2.3 Boundary Conditions *18*

2.4 Solutions *19*

2.4.1 Solution I *19*

2.4.2 Solution II *23*

2.5 Results and Discussion *24*

2.5.1 Comparison between Solution I and Solution II *24*

2.5.2 Sensitivity to the distance to the PRB (L_A) *from the contaminant source area* *26*

2.5.3 Sensitivity to the thickness of the PRB (L_B) *29*

2.5.4 Sensitivity to NAC inside PRB *31*

CHAPTER 3 33
DESIGN METHODOLOGY 33
3.1 Design Methodology I *33*
3.1.1 Fundamental components of model I *33*
3.1.1.1 Aquifer hydrodynamic dispersion coefficient (DA) *34*
3.1.1.2 Simplified Model I *35*
3.1.2 Standard curves *36*
3.1.3 Steps to the empirical design equation I *37*
3.1.4 Empirical Design Methodology I *44*
3.2 Design Methodology II *44*
3.3 Model Performance *45*
CHAPTER 4 ..... **47**
CASE STUDY 47
4-1. Problem Background *47*
4-2. Parameter estimation *49*
4-2-1 The natural attenuation capacity in the aquifer NAC_A estimation *49*
4-2-2 First-order decay rate inside the reactive barrier λ_B estimation *52*
4-2-3 Natural attenuation capacity in the PRB NAC_B estimation *52*
4-2-4 Estimation of LB-design *53*
REFERENCES *55*
CHAPTER 5 ..... **54**
ENGINEERING SIGNIFICANCE 54

APPENDIX A **56**

APPENDIX B **77**

LIST OF FIGURES

Figure 2-1: Conceptual model of a contaminant plume passing through a permeable reactive barrier. 17

Figure 2-2-a: Contaminant concentrations calculations using Solution I and Solution II -Example (a)- 24

Figure 2-2-b: Contaminant concentrations calculations using Solution I and Solution II - Example (b)- 25

Figure 2-3: Scenarios of a PRB placed at two different distances from the source of contamination 26

Figure 2-4-a: Contaminant concentrations calculations with 3 different values of L_A - Example (c)- 27

Figure 2-4-b: Contaminant concentrations calculations with 3 different values of L_A - Example (d)- 28

Figure 2-5-a: Example (e) of Concentrations of a Contaminant calculated upgradient, downgradient and within a PRB system using solutions of Model I and Model II, for different PRB thicknesses. 29

Figure 2-5-b: Example (f) of Concentrations of a Contaminant calculated upgradient, downgradient and within a PRB system using solutions of Model I and Model II, for different PRB thicknesses. 30

Figure 2-6: Example (g) - Concentrations of a Contaminant calculated upgradient, downgradient and within a PRB system using solutions of Model I, for different NAC_B^{nd} values 31

Figure 3-1 : PRB Design Curves Dk_{wall} $vs.$ $C_A^{std,\lambda_A} / C_s$ 37

Figure 3-2 : Dimensionless Correction Factor Φ_{λ_A} 38

Figure 3-3 : Dimensionless Correction Factor Ψ_{λ_A} 38

Figure 3-4: Parameter A_{VA} 41

Figure 3-5: Parameter B_{POC} 42

Figure 3-6: Empirical Design Equation performance 46

Figure 3-7: Analytical Design Equation performance 46

Figure 4-1: Map of San Francisco and vicinity (Battelle., 1998) 48

Figure 4-2 : Moffett Field solvent plume (Battelle., 1998) 48

Figure 4-3 : TCE concentration contour map (IT Corp., 1991) 49

Figure 4-4: Location of Model Boundaries and Monitoring Wells in the vicinity of the PRB (Battelle., 2005) 51

LIST OF TABLES

Table 1-1: Summary of five full-scale reactive barriers installed in the field (U.S. EPA Remedial Technology Fact Sheet, EPA/600/F-97/008) 7

Table 3-1: $\frac{C_A\left(L_{POC}, V_A, \lambda_A = 0.001 d^{-1}\right)}{C_A\left(L_{POC} = 400m, V_A, \lambda_A = 0.001 d^{-1}\right)}$ 39

Table 3-2: $\ln\left(\frac{C_A\left(L_{POC}, V_A = 0.1 m/d, \lambda_A = 0.001 d^{-1}\right)}{C_A^{std}}\right) \Big/ \ln\left(\frac{C_A\left(L_{POC}, V_A, \lambda_A = 0.001 d^{-1}\right)}{C_A\left(L_{POC} = 400m, V_A, \lambda_A = 0.001 d^{-1}\right)}\right)$ 40

Table 3-3: $\frac{C_A\left(L_{POC} = 400m, V_A, \lambda_A = 0.001 d^{-1}\right)}{C_A^{std}}$ vs. V_A 42

Table 4-1: Bench-scale Test Results and Design projection (Battelle et al., 1998) 52

Chapter 1

Introduction

1.1 Background

Groundwater is generally more reliable for use than surface water. In the United States, 56% of the population relies on groundwater for their drinking water (Van der Leeden et al.1990). However groundwater resources are vulnerable because any chemical that is easily soluble and that can penetrate the soil is a prime candidate for a groundwater pollutant. Chlorinated hydrocarbons and chromium are two of the most serious pollutants threats continuously released to the groundwater as a result of many industrial operations and waste disposal (Kjeldsen et al. 2001). Further, a significant majority of Americans live near industrialized population centers, which are typically located near groundwater supplies (Delleur, 1999).

The U.S Environmental Protection Agency (EPA) recently estimated that there are over 217,000 contaminated sites in the U.S with an associated cleanup cost of about $ 190 billion dollars (EPA, 1996).Constructed underground storage tank systems associated with petroleum fuel storage and dispensing at service stations and convenience stores as well as wood preservation,

electroplating and other industrial processes are increasingly used to satisfy the growing needs of different industries. Historical data suggests that, even with modern site construction techniques, materials, and leak detection systems, most of these systems will leak at some time and will go undetected (Miller, 2003). Consequently, the environment is constantly receiving spills and leaks of pollutants such as chlorinated solvents and hexavalant chromium. Chlorinate solvents such as perchlorethene (PCE), trichlorethene (TCE), and trichloroethane (TCA), present both in NAPL form (non-aqueous phase liquid; the bulk liquid chlorinated solvent) and also as dissolved contaminants in the groundwater are causing extensive contamination.

Groundwater remediation techniques such as pump and treat are widely used but have proven that they are difficult, costly and ineffective most of the time in removing enough contamination to restore the ground water to drinking water standards in acceptable time frames (Travis et al.1990; Gillham et al.1992; National Research Council, 1994). The primary reason for the failure of pump and treat is the inability to extract contaminants from the subsurface due to hydrogeologic factors and trapped residual contaminant mass. However, a recent remedial technique using Permeable Reactive Barriers (PRBs) is found to be more cost-effective than pump and treat and has been a demonstrated potential to diminish the spread of contaminants which have proven difficult and expensive to manage with other cleanup methods (Puls et al. 1998).

Previous research suggests that chlorinated hydrocarbons, and chromium are readily reduced using iron oxide, resulting in dechlorination of TCE and precipitation and immobilization of chromium (Simon et al. 2000), respectively. Consequently, the majority of PRBs already installed use granular iron media, although some organic materials are being used as reactive media to biologically remediate certain other contaminants, such as nitrate and sulfate (Puls et al. 1998). These barriers are installed perpendicular to the groundwater flow path and the contaminant plume to create a reactive treatment zone. Similarly, biologically active zones are created by

providing nutrients and microorganisms in high concentrations to create a reactive flow-through barrier (Puls et al. 1998).

The design of the PRB will vary depending on the pollutants being remediated. In principle, any pollutant that is chemically or biologically degradable can be treated within a properly designed and constructed reactive barrier. However, current design formulas are limited and do not properly account for all major physical and attenuation processes driving remediation. PRB design formulas are empirically based and have very narrow design objectives that tend to result to excessive wall thicknesses. Formulas for designing the thickness of a PRB do not account for the natural attenuation capacity of the aquifer; either upgradient between the source and the PRB or downgradient of the reactive wall. In addition, it does not include the point of regulatory compliance, where the concentration target is located downgradient of the source and the PRB. Thus, a new paradigm is needed for the design of PRB in conjunction with monitored natural attenuation (MNA) to achieve site-specific remediation objectives.

1.2 Natural Attenuation

Without human intervention, natural attenuation process can reduce the mass, toxicity, mobility, volume, or concentration of contaminants in soil or groundwater (U.S. EPA, 1999). This natural process is described in the National Oil and Hazardous Substances Pollution Contingency (NCP) as a process that will effectively reduce contaminants in the groundwater to concentrations protective of human health and sensitive ecological environments in a reasonable timeframe (U.S. EPA, 1990a). Under the appropriate conditions at some sites, natural attenuation can contribute significantly to remediation of dissolved chlorinated solvent contamination (U.S. EPA, 1990a). However, in areas with relatively high contaminant levels, the plume will require, most of the time, a much longer time to attenuate naturally. The EPA directive on MNA does not advocate for a

reliance on MNA as an individual remediation technology and has stressed that in the majority of cases where monitored natural attenuation is proposed as a remedy, its use may be appropriate as one component of the total remedy, that is, either in conjunction with active remediation or as a follow-up measure (U.S. EPA, 1997, p.1).

Therefore, for the majority of sites, it is thought that MNA alone is not capable of reaching desired cleanup levels in a reasonable timeframe but natural attenuation combined with more active remediation methods may prove to be effective to achieve cleanup goals within a reasonable timeframe in order to achieve remedial objectives (Lovelace et al. 1997). Source remediation technologies (e.g., chemical oxidation) for partial contaminant source removal are used in conjunction with MNA to reach site-specific remedial action objectives. Chapelle et al. (2005) demonstrated this approach at a chlorinated solvent-contaminated site in the U.S. Atlantic Coast Plain in Georgia where plume reduction was documented over a 6-year period. One promising technology is the Barrier-Controlled MNA approach that integrates three existing remediation strategies (source containment, monitored natural attenuation, and, if necessary, engineered source reduction) developed by Filz et al. (2001). This technique significantly reduces the risk caused by exposure to contaminated groundwater and the cost of remediation.

1.3 Zero-Valent Iron

In the natural environment, many contaminants are degraded as a result of chemical reactions and biological transformations of the substances. In recent years, research has shown that metals can react with certain chemicals and can change their form. A well known example that advanced the progress of organic chemistry is the discovery of the Grignard reaction, an organometallic chemical reaction involving alkyl- or aryl-magnesium halides, also called Grignard reagents which won the French chemist Victor Grignard the Nobel Prize in 1912 (Powell et al.

1998). From the same source, in 1980 for example, Sweeney patented the use of iron metal to reduce certain hydrocarbons in aqueous waste streams and in 1982 Gould investigated metallic iron as a reductant for Cr(VI) at pH<5 in wastewaters and proposed reaction mechanisms. In 1987, Hagenmaier and colleagues observed that copper has catalytic effects on the decomposition of polychlorinated dibenzo-p-dioxins (PCDD) and polychlorinated dibenzofurans (PCDF) and on other polychlorinated aromatic (Powell et al. 1998).

Ito and Kimura (1997) concluded that many chlorinated solvents, such as TCE or PCE could be degraded by IP (iron powder) in aqueous solution and that weak acide reductants, like sodium hydrogen sulfite (NaSO3), could contribute to a degradation of TCE and PCE with IP. In the contact of iron surfaces, polluting compounds; such as, halogenated compounds and pesticides are degraded abiotically as it is detailed in Gillham and O'Hannesin (1994) and Sweeny and Fisher (1972) respectively and chromate are degraded to a less mobile and toxic compound as it is detailed in Blowes et al. (1997).

1.4 Permeable Reactive Barriers

A permeable reactive subsurface barrier has been defined as: "...an emplacement of reactive materials in the subsurface designed to intercept a contaminant plume, provide a flow path through the reactive media, and transform the contaminant(s) into environmentally acceptable forms to attain remediation concentration goals downgradient of the barrier." (Powell et al. 1998). PRBs are designed as conduits for the contaminated groundwater flow corresponding to screens to contaminants, but not to groundwater flow. When contaminated water passes through the reactive zone of the PRB, the contaminants are either stopped or transformed to new chemical entities less toxic or more readily biodegradable. Water permeable treatment walls are assumed to be installed as permanent, semi-permanent, or replaceable units across the flow path of a contaminant plume,

allowing the plume to move passively through while precipitating, sorbing, or degrading the contaminants (In Situ Remediation Technology Status, EPA, 1995).

There are currently around 15 pilot and full-scale permeable reactive wall projects being demonstrated (U.S. EPA, 2002). The EPA has officially recommended the use of permeable reactive barrier technology by saying that it has the potential to more effectively remediate subsurface contamination at many types of sites at significant cost savings compared to other more traditional approaches (U.S. EPA, 1997). The EPA has suggested that they can be used at up to 20% of the chlorinated compound contaminated sites. Table 1 is showing five full-scale reactive barriers installed in the field for the treatment of plumes of chlorinated hydrocarbons and chromate (Puls et al. 1997).

Reactive barriers were originally developed in the US to enhance the process of degradation of chlorinated solvents. PRBs have materials embedded in them that can enhance degradative reactions. The first applications involved the use of elemental iron, FeO, to catalyze the dechlorination of PCE and TCE, although it was found that vinyl chloride could be produced. Refinement of the technique has reduced this problem, but it is common practice to use a reactive barrier of this type in combination with a passive oxygen releasing system located down gradient of the wall (Byerley et al. 1996). This helps to ensure that reductive conditions are present within the wall, but aerobic conditions are present downgradient to enhance the degradation of any residual breakdown products. One of the recent experimentation with these techniques has involved the use of elemental rubidium and platinum, which are more effective catalysts.

Table 1-1: Summary of five full-scale reactive barriers installed in the field (U.S. EPA Remedial Technology Fact Sheet, EPA/600/F-97/008)

Site	Industrial facility, Mountainview California	Industrial facility, Belfast, Northern Ireland	Industrial facility, Coffeyville, Kansas	USCG facility, Elizabeth City, North Carolina	Government facility, Lakewood, Colorado
Installation date	Sept. 1995	Dec. 1995	Jan. 1996	June 1995	Oct. 1996
Contaminant & high conc. Design	2 mg/L cDCE	300 mg/L TCE	400 µg/L TCE	10 mg/L TCE 10 mg/L Cr(VI)	700 µg/L each TCE & DCE 15 µg/L VC
Reactive Wall Type	Excavate & fill	Reaction Vessel	Funnel & Gate	Continuous Trench	Funnel & Multiple Gate
Funnel Material	Not Applicable	Slurry Walls	Soil-Bentonite Slurry	Not Applicable	Sealable Joint Sheet Pilings
Funnel Length	Not Applicable	100 ft + 100 ft	490 ft + 490 ft	Not Applicable	1040 ft total
No. Of Gates	Not Applicable	1 Reaction vessel	1	Not Applicable	4
Reactive Material	Fe metal	Fe metal	Fe metal	Fe metal	Fe metal
Reactive Zone Height	5 ft	16 ft in vessel	11 ft	Approx. 23 ft	10-15 ft
Reactive Zone Length	44 ft	NA	20 ft	150 ft	40 ft each (4 x 40 = 160)
Reactive Zone Thickness	4.5 ft	16 ft in vessel	3 ft	2 ft	Gates differed, low = 2 ft high = 6 ft
Total Mass of Reactant	90 tons	15 tons	70 tons	450 tons	No Information
Treatment Wall Depth	15 to 20 ft bgs	18 to 40 ft bgs	17 to 28 ft bgs	3 to 26 ft bgs	10-15 to 20-25 ft bgs
Total System Length	44 ft	Approx. 200 ft	1000 ft	150 ft	1200 ft
Special Features &Mis.	HDPE atop Fe to surface upgradient directs H2O through Fe	Walls direct H2O to vessel inlet, gravity flow to outlet downgradient		Two contam. treated. Chain trencher with immediate Fe placement	Largest of its kind. Gates installed using sheet pile box.
Cost	No Information	$375 K	$400 K	$500 K	No Information

Most of the 26 PRB systems in the US have used granular iron media and have been applied to address the control of contamination caused by chlorinated volatile organic compounds or heavy metals.(U.S. EPA , RTDF, 2001). Although it is hard to tell for sure whether these systems put in place will reach in the long-term the performances needed, many of them already showed satisfaction on remediating the contamination. However, some of the systems showed bad performances.

In June 1996, a permeable subsurface reactive wall composed of granular iron, 46 meter long, 7.3 meter deep and 0.6 meter wide was installed at the U.S. Coast Guard Support Center (USCG) in Elizabeth City, North Carolina proved to remediate the hexavalent chromium [Cr(VI)] groundwater plume via reduction and precipitation processes and dechlorinate portions of a larger trichloroethylene (TCE) groundwater plume at the site (Blowes et al. 1999).

In September 1997, at the Fry Canyon of the state of Utah experimental site, in order to reduce the uranium concentrations in the groundwater to less than 10 parts per billion, three PRBs containing foamed zero-valent iron (ZVI) pellets, bone charcoal pellets and amorphous ferric oxyhydroxide (AFO) slurry mixed with pea gravel, were installed. After 1 year of operation, the conclusion was that the zero-valent iron (ZVI) permeable barrier was much more effective than bone charcoal pellets and amorphous ferric oxyhydroxide (AFO) and has removed more than 99.9% of the uranium (U.S. Geological Survey, 1997).

In 1999, at the Cape Canaveral Air Force Station in Florida, the site with very low hydraulic gradient (0.01%) was contaminated with about 20,000 kg of DNAPL, mostly TCE and derived products present in the site with concentrations as high as 3 mg/L for TCE and as high as 30 mg/L for cis-1,2-dichloroethene (DCE). A reactive wall with dimensions of 12.2 m deep, 12.2 m wide and 1.2 m thick constituted of Eleven 12.2-m long 1.2- m diameter overlapping columns containing 16 wt.% ZVI, 79 wt.% native soil and 5 wt.% gravel was installed and had successfully degraded

influent TCE to nondetectable levels except in one downgradient monitoring well where the concentrations have been steadily declining since May 1999 but are still above the MCLs (Reinhart et al. 2000).

In August 1999, at the Pease Air Force Base of New Hampshire a PRB was installed using a biopolymer slurry technique where the total VOC concentration exceeded 1,000 mg/L and the site was contaminated with TCE and daughter. A total of 487 tons of sand and 359 tons of granular (-8 to +50 U.S. mesh size) iron were installed in a trench that generated 473 yd^3 of spoils. In order to improve hydraulic conductivity of the barrier, 20 gal of enzyme were injected into the barrier through a 6-in PVC flushing well to help in the degradation of biopolymer. The contaminants were degraded inside the wall (Cange et al. 2000).

In 1998, a full-scale PRB system at the Caldwell Trucking Superfund Site in northern New Jersey was installed at 915m downgradient of the source area to reduce initial TCE concentrations of 6,000- 8,000 µg/L in the groundwater to below 50 µg/L prior to discharge to surface water. The site was contaminated mainly by TCE because of a big area near the Passaic River was used for disposal of septic wastes in unlined ponds from the 1950s to 1984 and industrial waste containing lead and TCE. The natural attenuation occurring at this site was said to be around 3,000 kg/yr. The system put in place consists of two 7.6-cm walls, 46 m and 27.4 in length and uses 250 tons of ZVI as the reactive material. The barrier until now is not achieving the performance for which it was designed for, which degraded only 50% degradation of TCE in the groundwater, from an upgradient concentration of 7,000 µg/L to a downgradient concentration of less than 3,500 µg/L. The low performance of this PRB is said to be a consequence of a change in the groundwater flow regime because of the reduction of the hydraulic conductivity of the fractures from the infilling with granular iron resulting from the injection of granular iron into the fractured bedrock, and, also of

the high pH and low temperature at which the guar gum gel used for the iron installation slowed its breaking when in place.

Because of the fact that metals can react with certain chemicals and change their forms which make the contaminants capable to degrade as a result of chemical reactions and biological transformations of their constituents, a technique that uses a combination of PRM and MNA in appropriate situations may represent a more sustainable solution to remediate cost-effectively any contaminations.

1.5 Existing Design Methodologies for PRBs

There are only a few PRB design methodologies to determine the thickness of a PRB documented in literature. The Environment Agency of UK (National Groundwater & Contaminated Land Centre report, 2002) proposed estimating wall thickness using the following equation, based on treatment process that can be described as a first order reaction:

$$L_B = t_{res} * V_B * S_F \qquad \text{..... (1-1)}$$

and

$$t_{res} = -\frac{\ln(C_T / C_0)}{k} \qquad \text{..... (1-2)}$$

where C_T = concentration target (µg/l); C_0 = concentration at source(µg/l); t_{res} = time of residence in the wall (d); V_B = velocity of the water (m/d); k = reaction rate (d^{-1}); and S_F = safety factor.

The previous design formula attempts to have the target concentration at the exit of the barrier and not at the point of compliance. The formula also does not account for dispersion.

Neglecting dispersion, a commonly used assumption in PRB analysis, can lead to non-conservative designs (Rabideau et al.2005). The reactive wall in most cases will be installed near the source of pollution to contain the majority of the pollutant and consequently this formula overestimates the thickness of the barrier. Additionally, this formula does not account for the natural attenuation capacity of the aquifer and uses a factor of safety that adds inadequacy to the formula.

Rabideau et al. proposed a set of improved analytical models for the design of Iron-based PRBs in their November 2005 paper. Although the proposed equations included the effects of dispersion, sequential decay and production processes, the study neglected the natural attenuation mechanism that is responsible in degrading the contaminant further when in contact with the aquifer which leads to overestimating the thickness of the PRB. Also, the study provides a methodology to calculate the thickness of the PRB through a complicated optimization approach.

References

Archer, W.L.; Simpson, E.L. Ind. Eng. Chem.*1977, 16(2), 158-162*

Borden, R.C. ;R.D. Norris; R.E. Hinchee; R. Brown; P.L. McCarty; L. Semprini; J.T. Wilson; D.H. Campbell; M. Reinhard; E.J. Bouwer; R.C. Borden; T.M. Vogel; J.M. Thomas; C.H. Ward eds. Natural Bioremediation of Hydrocarbon-Contaminated Ground Water. *Handbook of Bioremediation*, Lewis Publishers, Boca Raton, FL. 1994.

Blowes D.W.; C.J. Ptacek; J.L. Jambor. In-situ remediation of Cr(VI)-contaminated groundwater using permeable reactive walls: Laboratory studies. *Environ. Sci. Technol. 1997. 31(12), 3348-3357.*

Blowes D. W. et al. An in situ permeable reactive barrier for the treatment of hexavalent chromium and trichloroethylene in groundwater. Volume 2, Performance Monitoring, *U.S. EPA Report EPA/600/r-99/095b (U.S. EPA, Office of Research and Development, Washington, September 1999).*

Byerley, B. T., Chapman, S. W. Smyth, D. J. A. & Mackay, D. M. A pilot test of passive oxygen release for enhancement of in-situ bioremediation of BTEX-contaminated ground water. manuscript in submission.*1996*

Cange, J. Installation of Permeable Reactive Wall at Pease Air Force Base Using Biopolymer Slurry Technique: Presented at RTDF Permeable Barriers Action Team Meeting*. February 16-17, 2000, Melbourne.*

Chapelle, F.H., P.M. Bradley, and C.C. Casey. 2005. Behavior of a chlorinated ethene plume following source-area treatment with Fenten's reagent. *Ground Water Monitoring and Remediation* 25, no. 2: 131-141

Daniel, F. P; J. N. Jones. Monitored Natural Attenuation of Chlorinated Solvents.*EPA.1999*

Filz,M.G.; M.A.Widdowson; J.C.Little .Barrier-Controlled Monitored Natural Attenuation. *Environ.Sci. Technol. 2001.*

F. van der Leeden, F. L. Troise, D. K. Todd, The Water Encyclopedia (Lewis, Chelsea, MI, 1990).

Gillham, R. W.; S. F. O'Hannesin. Enhanced Degradation of
Halogenated Aliphatics by Zero-Valent Iron. *Ground Water. Vol. 32, No. 6,
pp958-967.1994*

Gillham, R.W; D.R.Burris. Recent developments in permeable in situ treatment walls for remediation of contaminated groundwater. *Proceedings, Subsurface Restoration Conference, June 21-24, Dallas, Texas. 1992*

Hocking, G. Vertical Hydraulic Fracture Emplacement of PRBs. *Presented at RTDF Permeable Barriers Action Team Meeting, April 15-16, 1998, Beaverton, OR.*

Ito, H.; T. Kimura; J.J. Liskowitz. The Reductive dechlorination of Chlorinated Compounds Using Iron Powder. *American Chemical Society. 1997.*

Kjeldsen, P.; T. Locht; P. Karvonen. Removal of TCE and Chromate in a Permeable Reactive Barrierusing Zero-Valent Iron.*2001.1*

Lovelace, K.; P. Feldman. Proceedings of the Symposium on Natural Attenuation of Chlorinated Organics in Ground Water.*EPA.1997.*

Miller,D.K.;P.C.Johnson;C.Bruce. Bioremediation of MTBE utilizing Permeable Reactive Barrier Technology. *Naval Facilities Engineering Service Center.*

National Research Council. Alternatives for ground water cleanup. *National Academy Press, Washington, D.C., 315 p. 1994*

Puls, R. W. Subsurface Protection and Remediation Division, NRMRL, ORD, U.S. EPA

Puls, R. W.; R. M. Powell; D. W. Blowes; J. L. Vogan; D. Schultz; T. Sivavec; P. D. Powell; R. Landis. Permeable Reactive Barrier Technologies For Contaminant Remediation. *U.S. EPA .1998*

Powell,R.M. Powell & Associates Science Services, Las Vegas, NV

Rabideau, A.J.; R. Suribhatla; J. R. Craig. Analytical Models for the Design of Iron-Based Permeable Reactive Barriers. *November2005.*

Reinhart, D.R.; M.B. Chopra; C.A. Clausen; J. Quinn. NASA PRB Installation using Deep- Soil Mixing:Presented at RTDF Permeable Barriers Action Team Meeting. *February 16-17, 2000,Melbourne, FL.*

Simon F.; T. Meggyes. Removal of organic and inorganic pollutants from groundwater using permeable reactive barriers *Published in Land Contamination & Reclamation, Vol. 8, Issue 2, 103-116 (2000)*

Smith, J. National Groundwater &Contaminated Land Center, Environment Agency

Sweeny, K. H.; J. R. Fisher. Reductive Degradation of Halogenated Pesticides.*1972.U.S. Patent No. 3,640,821.*

Travis, C.C., and Doty, C.B. 1990. Can contaminated aquifers at Superfund sites be remediated?. Environmental Science and Technology. 24:1464-1466.

U.S. Environmental Protection Agency. Field Applications of In Situ Remediation Technologies: Permeable Reactive Barriers. *2002*

U.S. Environmental Protection Agency. Remediation Technologies Development Forum. www.rtdf.org/public/permbarr/PRBSUMMS. April 2001

U.S. Environmental Protection Agency. Use of Monitored Natural Attenuation at Superfund, RCRA corrective action, and underground storage tank sites. *April 1999*

U.S. Environmental Protection Agency. Office of Solid Waste and Emergency Response Directive 9200. Use of Monitored Natural Attenuation at Superfund, RCRA Corrective Action, and Underground Storage Tanks. *1997.*

U.S.Environment Protection Agency. Cleaning Up the Nation's Waste Sites: Markets and Technology Trends. *Edition EPA 542-R-96-005A.1997.*

U.S. Environmental Protection Agency. National Oil and Hazardous Substances Pollution Contingency Plan: Final rule (NCP). *Fed. Reg.55(46):8733-8734. 1990a*

U.S. Geological Survey ,U.S. Bureau of Land Management ,U.S. Department of Energy .Field Demonstration Of Permeable Reactive Barriers To Remove Dissolved Uranium From Groundwater, Fry Canyon, Utah. .*p 1-2.1997*

Wiedemeier, T.H.; M.A., Swanson; D.E.; Moutoux; E.K Gordon; J.T Wilson; B.H Wilson; D.H Kampbell; J.E. Hansen; P. Haas; F.H. Chapelle.. *Technical Protocol for Evaluating Natural Attenuation of Chlorinated Solvents in Ground Water. p 1-5. Air Force Center for Environmental Excellence, Brooks Air Force Base, San Antonio, TX. 1997*

Wycisk, P.; Weiss H.; Kaschl A.; Heidrich S.; Sommerwerk K. Groundwater pollution and remediation options for multi-source contaminated aquifers (Bitterfeld/Wolfen, Germany). *2002*

Vidumsky, J. Permeable Barrier Remedy Performed at Caldwell Trucking Site. *Presented at RTDF Permeable Barriers Action Team Meeting, April 15-16, 1998, Beaverton, OR. 1998*

Chapter 2

Mathematical Model and Solutions

2.1 Objective

The goal of this research was to set up a methodology to design PRBs that are easy to implement while improving accuracy and being more conservative than the available design methodologies.

Four research objectives are identified:

1- Solve mathematically the system of 1) a one-dimensional governing equation of contaminant transport through a PRB governed by advection, dispersive mass flux, and a first-order permeable reactive barrier decay-rate and 2) a one-dimensional governing equation of the contaminant transport through the receiving aquifer governed by advection, hydrodynamic dispersion, and a first-order biodegradation decay-rate, using total contaminant mass flux and interface boundary conditions between the PRB and the aquifer.

2- Create a database of 7,500 hypothetical cases using the solutions of the PRB conceptual model and set up an empirical equation to calculate the thickness of the PRB capable of degrading a contaminant from a source contaminant concentration C_s to a maximum contaminant level C_{MCL} at a Point of compliance POC

3- Investigate particular solutions that translate the assumption that the contaminant is reduced due to the reactive capacity of the PRB only when it travels within the PRB and is reduced due to the natural attenuation process only when it travels outside of the PRB against the solutions developed in step 1 to determine whether or not they are good substitutes to the more complex solutions of the PRB mathematical system, and if they are

4- generate an analytical design equation using the particular solutions and investigate its performance against the performance of the empirical equation to determine the best methodology to design PRBs.

2.2 Governing Equations

The following mathematical model is for a simplified, one-dimensional, steady-state representation of dissolved contaminants moving by advection and dispersion in an aquifer. Natural attenuation reduces the concentration along the flow path until reaching a PRB, where contaminants are provided a flow path through the reactive media. In the PRB, contaminants are degraded more efficiently. Downgradient of the PRB, the natural attenuation of the aquifer reduces the contaminant concentration.

The 1-D model consists of the source area (where the aqueous-phase source is assumed to be perfectly mixed and the concentration, C_S, is assumed to be uniform) and two homogenous, porous transport domains: the receiving aquifer and the permeable reactive barrier (Figure 2-1). Because the reactive barrier is permeable, flow velocity, v_B, in the barrier is such that flow rate entering the reactive barrier stay constant

$$V_A n_A = V_B n_B \qquad \text{..... (2-1)}$$

where n_A =effective porosity of the aquifer [L^3/ L^3]; n_B =effective porosity of the barrier [L^3/ L^3]; and V_A =flow velocity in the aquifer.

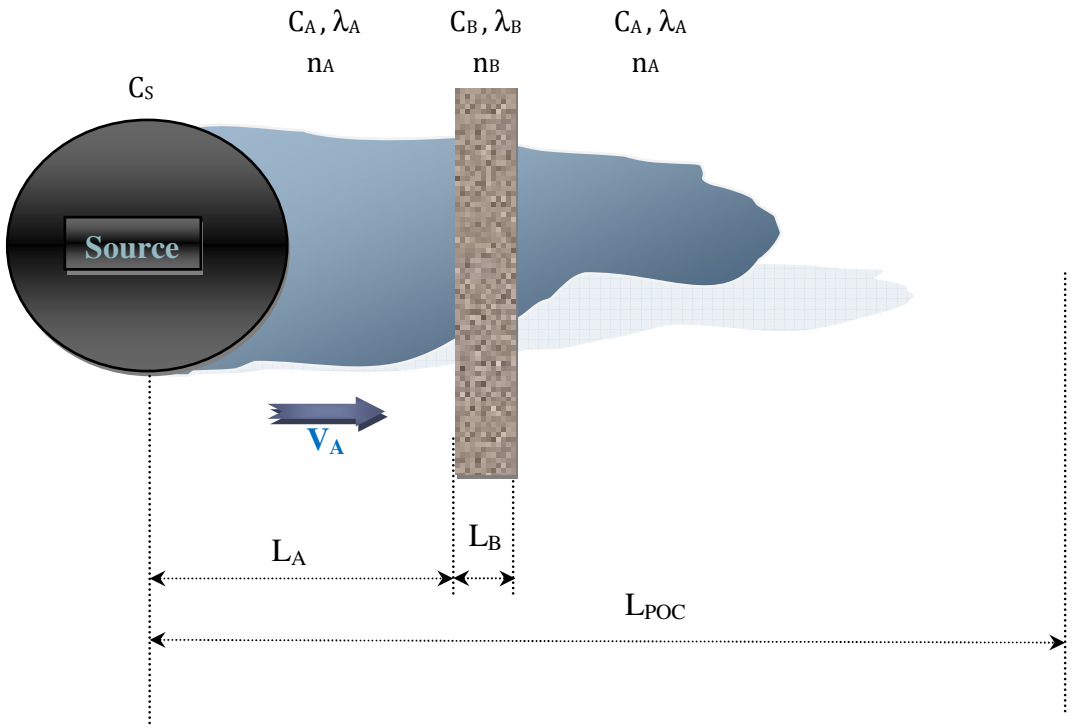

Figure 2-1: Conceptual model of a contaminant plume passing through a permeable reactive barrier.

Contaminant transport inside the barrier is the sum of the advection, dispersive mass flux, and a first-order permeable reactive barrier decay-rate, and

$$D_B \frac{\partial^2 C_B}{\partial x^2} - V_B \frac{\partial C_B}{\partial x} - \lambda_B C_B = 0 \qquad \text{..... (2-2)}$$

where C_B is the aqueous-phase concentration [M/L^3] in the permeable reactive barrier for $L_A \le x \le L_A + L_B$; D_B is the reactive barrier molecular dispersion coefficient [L^2/T]; and λ_B is the first-order reactive barrier rate constant [T^{-1}]. Solute transport in the aquifer is governed by advection, hydrodynamic dispersion, and a first-order biodegradation decay-rate, or

$$D_A \frac{\partial^2 C_A}{\partial x^2} - V_A \frac{\partial C_A}{\partial x} - \lambda_A C_A = 0 \qquad \text{..... (2-3)}$$

where C_A is the aqueous-phase concentration [M/L^3] in the aquifer for $0 \le x \le L_A$ and for $L_A \le x < \infty$; D_A is the hydrodynamic dispersion coefficient [L^2/T]; and λ_A is the first-order biodegradation rate constant [T^{-1}]. Continuity is assumed at the reactive barrier- aquifer interface.

2.3 Boundary Conditions

The mathematical model consists of the three governing differential equations describing solute transport in the aquifer upstream of the barrier, in the barrier, and in the aquifer downstream of the barrier (Equations 2-2 and 2-3), two boundary conditions:

$$C_A(0) = C_s \qquad \text{.....(2-4a)}$$

$$C_A(x \to \infty) = 0 \qquad \text{.....(2-4b)}$$

and four intermediate conditions at the interface between the barrier and the aquifer:

$$C_A = C_B \text{ at } x = L_A \qquad \text{.....(2-5)}$$

$$C_A = C_B \text{ at } x = L_A + L_B \qquad \text{.....(2-6)}$$

$$-D_B n_B \frac{\partial C_B}{\partial x} + V_B n_B C_B = -D_A n_A \frac{\partial C_A}{\partial x} + V_A n_A C_A \text{ at } x = L_A \qquad \text{.....(2-7)}$$

$$-D_B n_B \frac{\partial C_B}{\partial x} + V_B n_B C_B = -D_A n_A \frac{\partial C_A}{\partial x} + V_A n_A C_A \text{ at } x = L_A + L_B \qquad \text{.....(2-8)}$$

where L_A is the distance from source of contaminant to the reactive barrier and L_B is the thickness of the reactive barrier.

Equation 2-7 equates the total contaminant mass flux entering the reactive barrier to the total contaminant mass flux leaving the aquifer at the upstream barrier-aquifer interface, and Equation 2-8 equates the total contaminant mass flux leaving the reactive barrier to the total contaminant mass flux reentering the aquifer at the downstream barrier-aquifer interface.

2.4 Solutions

2.4.1 Solution I

Three dimensionless distance variables can be defined

$$X_U = \frac{x}{L_A} \qquad \text{.....(2-9a)}$$

$$X_B = \frac{x - L_A}{L_B} \qquad \text{.....(2-9c)}$$

$$X_D = \frac{x - L_A - L_B}{L_{POC} - L_A - L_B} \qquad \text{.....(2-9b)}$$

where X_U is dimensionless distance in the aquifer upstream of the reactive barrier $(0 \le X_U \le 1)$; X_B is dimensionless distance in the reactive barrier $(0 \le X_B \le 1)$; X_D is dimensionless distance in the aquifer downstream of the reactive barrier $0 \le X_D < \infty$; and L_{POC} is the distance from source of contaminant to POC. The distance L_{POC} is a site-specific characteristic length associated with the aquifer.

The solution to Equation 2-2, 2-3 (Appendix A) can be expressed in a dimensionless form for each of the three domains:

1. For $0 \le X_U = \frac{x}{L_A} \le 1$

$$C_A^R(X_U) = C_2 \exp(NAC_A^{nd} X_U) + (1 - C_2) \exp(\overline{NAC_A^{nd}} X_U) \qquad \text{.....(2-10)}$$

2. For $0 \le X_B = \frac{x - L_A}{L_B} \le 1$

$$C_B^R(X_B) = C_3 \left(\exp(NAC_B^{nd} / L_B^R) * \exp(NAC_B^{nd} X_B) + C_1 \exp(\overline{NAC_B^{nd}} / L_B^R) * \exp(\overline{NAC_B^{nd}} X_B) \right) \text{...}$$

....(2-11)

3. For $0 \le X_D = \frac{x - L_A - L_B}{L_{POC} - L_A - L_B} \le 1$

$$C_A^R(X_D) = C_4 \exp\left(NAC_A^{nd}(1 + L_B^R)\right) * \exp(NAC_A^{nd} L_{POC}^R X_D) \qquad \text{.....(2-12)}$$

where C_A^R = relative concentration in the aquifer $= C_A / C_s$ and C_B^R = relative concentration in the reactive barrier $= C_B / C_s$. Equations 2-10, 2-11, and 2-12 are expressed in terms of six dimensionless groups

$$NAC_A^{nd} = \frac{1}{2}\left[P_e^A - \sqrt{(P_e^A)^2 + 4Dk_A P_e^A}\right] = \text{aquifer NAC} \qquad \text{.....(2-13)}$$

$$\overline{NAC}_A^{nd} = \frac{1}{2}\left[P_e^A + \sqrt{(P_e^A)^2 + 4Dk_A P_e^A}\right] = \text{aquifer conjugate NAC} \quad \text{.....(2-14)}$$

where $P_e^A = \frac{L_A v_A}{D_A}$ = aquifer Peclet number; and $Dk_A = \frac{\lambda_A L_A}{V_A}$ = aquifer Damkohler number, group I

$$NAC_B^{nd} = \frac{1}{2}\left[P_e^B - \sqrt{(P_e^B)^2 + 4Dk_B P_e^B}\right] = \text{NAC inside PRB} \quad \text{.....(2-15)}$$

$$\overline{NAC}_B^{nd} = \frac{1}{2}\left[P_e^B + \sqrt{(P_e^B)^2 + 4Dk_B P_e^B}\right] = \text{conjugate NAC inside PRB} \quad \text{.....(2-16)}$$

where $P_e^B = \frac{L_B v_B}{D_B}$ = barrier wall Peclet number; and $Dk_{wall} = \frac{\lambda_B L_B}{V_B}$ = reactive barrier Damkohler number, group I

$$L_B^R = \frac{L_B}{L_A} \quad \text{.....(2-17)}$$

$$L_{POC}^R = \frac{L_{POC} - L_A - L_B}{L_A} \quad \text{.....(2-18)}$$

$$\delta_A = \frac{1}{2}\left(1 - \sqrt{1 + 4\frac{Dk_A}{P_e^A}}\right) \text{ and its conjugate } \overline{\delta_A} = \frac{1}{2}\left(1 + \sqrt{1 + 4\frac{Dk_A}{P_e^A}}\right) \quad \text{.....(2-19)}$$

$$\delta_B = \frac{1}{2}\left(1 - \sqrt{1 + 4\frac{Dk_B}{P_e^B}}\right) \text{and its conjugate } \overline{\delta_B} = \frac{1}{2}\left(1 + \sqrt{1 + 4\frac{Dk_B}{P_e^B}}\right) \quad \text{.....(2-20)}$$

and four dimensionless coefficients:

$$\mathrm{C}_1 = \left(\frac{\delta_A - \delta_B}{\delta_A - \overline{\delta_B}}\right) * \exp\left(-(1+1/L_B^R)\sqrt{P_e^{B^2} + 4Dk_B P_e^B}\right) \quad \text{.....(2-21)}$$

$$\mathrm{C}_2 = \mathrm{C}_2' + \frac{C_1 C_2'''}{C_s} \quad \text{.....(2-22a)}$$

With $$C_2' = \frac{1}{C_2'' - 1} \quad \text{.....(2-22b)}$$

$$C_2'' = \frac{1 + \exp\left(-\sqrt{P_e^{B^2} + 4Dk_B P_e^B}\right)}{\left(\left(\frac{\delta_B - \overline{\delta_A}}{\delta_B - \delta_A}\right) + \left(\frac{\delta_B - \delta_A}{\delta_B - \overline{\delta_A}}\right) * \exp\left(-\sqrt{P_e^{B^2} + 4Dk_B P_e^B}\right)\right) * \exp\left(\sqrt{P_e^{A^2} + 4Dk_A P_e^A}\right)} \quad \text{.....(2-22c)}$$

$$C_2''' = \frac{1 + C_1 \exp\left(\frac{\sqrt{P_e^{B^2} + 4Dk_B P_e^B}}{L_B^R}\right)}{\exp\left(\overline{\delta_A} P_e^A - \frac{\overline{\delta_B} P_e^B}{L_B^R}\right) * \left(\begin{array}{l} \left(1 - \frac{\overline{\delta_A}}{\delta_B}\right) - \left(1 - \frac{\delta_A}{\delta_B}\right) \exp\left(-\sqrt{(P_e^A)^2 + 4Dk_A P_e^A}\right) + \\ C_1 \exp\left(\frac{\sqrt{P_e^{B^2} + 4Dk_B P_e^B}}{L_B^R}\right) * \left(\left(\frac{\overline{\delta_B} - \overline{\delta_A}}{\delta_B}\right) - \left(\frac{\overline{\delta_B} - \delta_A}{\delta_B}\right) \exp\left(-\sqrt{(P_e^A)^2 + 4Dk_A P_e^A}\right)\right) \end{array}\right)} \quad \text{....(2-22d)}$$

$$C_3 = \frac{C_2 \exp\left(\frac{1}{2}\left(P_e^A - \sqrt{(P_e^A)^2 + 4Dk_A P_e^A}\right)\right) + (1 - C_2) \exp\left(\frac{1}{2}\left(P_e^A + \sqrt{(P_e^A)^2 + 4Dk_A P_e^A}\right)\right)}{\exp\left(\frac{P_e^B - \sqrt{(P_e^B)^2 + 4Dk_B P_e^B}}{2L_B^R}\right) + C_1 \exp\left(\frac{P_e^B + \sqrt{(P_e^B)^2 + 4Dk_B P_e^B}}{2L_B^R}\right)} \quad \text{....(2-23)}$$

$$C_4 = \frac{C_3\left(\exp\left(\frac{1}{2}\left(P_e^B - \sqrt{(P_e^B)^2 + 4Dk_B P_e^B}\right) * \left(1 + \frac{1}{L_B^R}\right)\right) + C_1 \exp\left(\frac{1}{2}\left(P_e^B + \sqrt{(P_e^B)^2 + 4Dk_B P_e^B}\right) * \left(1 + \frac{1}{L_B^R}\right)\right)\right)}{\exp\left(\frac{1}{2}\left(P_e^A - \sqrt{(P_e^A)^2 + 4Dk_A P_e^A}\right) * (1 + L_B^R)\right)} \quad \text{....(2-24)}$$

2.4.2 Solution II

Particular solutions to the system of differential Equations 2-2 and 2-3 are obtained by assuming that the contaminant is reduced only by the reactive capacity of the PRB when it travels within the PRB and reduced only by the natural attenuation process when it travels along the aquifer either upgradient or downgradient from the PRB. The contaminant concentration is assumed to be:

- 1) a function $C_1 \exp(NAC_A^{nd} X_U)$ upgradient or downgradient from the PRB, where C_1 is a constant to be determined using the boundary conditions and,
- 2) a function $C_2 \exp(NAC_B^{nd} X_D)$ inside the PRB, where C_2 is also a constant to be determined using the boundary conditions.
- 3) equal to the contaminant concentration C_{MCL} when it reaches the point of compliance or when $X_D = 1.0$

$$C_A = C_{MCL} \text{ at } x = L_{POC} \qquad \text{.....(2-29)}$$

Using the continuity equations at the barrier-aquifer interface 5 and 6; and Equation 2-29, the solutions, expressed in a dimensionless form, are as follows:

$$C_A^R(X_U) = \exp(NAC_A^{nd} X_U) \qquad \text{.....(2-30)}$$

$$C_B^R(X_U) = \exp(NAC_A^{nd}) * \exp(NAC_B^{nd} X_B) \qquad \text{.....(2-31)}$$

$$C_A^R(X_D) = C_{MCL}^R \exp\left(NAC_A^{nd} L_{POC}^R (X_D - 1)\right) \qquad \text{.....(2-32)}$$

where $C_{MCL}^R =$ relative maximum contaminant level at point of compliance $= C_{MCL}/C_s$.

2.5 Results and Discussion

2.5.1 Comparison between Solution I and Solution II

In order to compare Solution I with the approximated Solution II, two different hypothetical examples (a) and (b) were used. Both examples were randomly picked from many examples that showed a reduction of the contaminant concentration to the concentration C_{MCL} of $5\mu g/l$ at their respective $POCs$ when Solution I was applied. Using the $5\mu g/l$ as a concentration C_{MCL}, Solution II was used for the same examples to calculate the contaminant concentrations at different locations upgradient, downgradient, and within the PRB. Figure 2-2a and Figure 2-2b below present the results of the calculations.

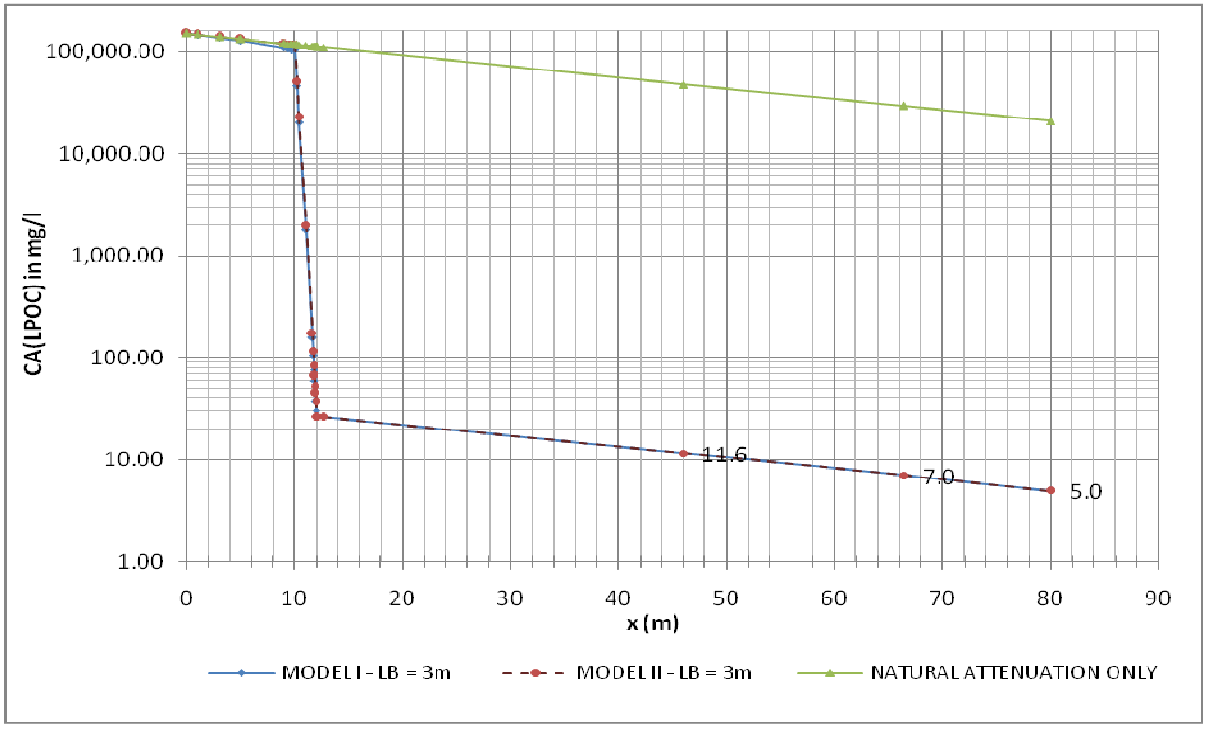

Figure 2-2 a: Contaminant concentrations calculations using Solution I and Solution II - Example (a)-

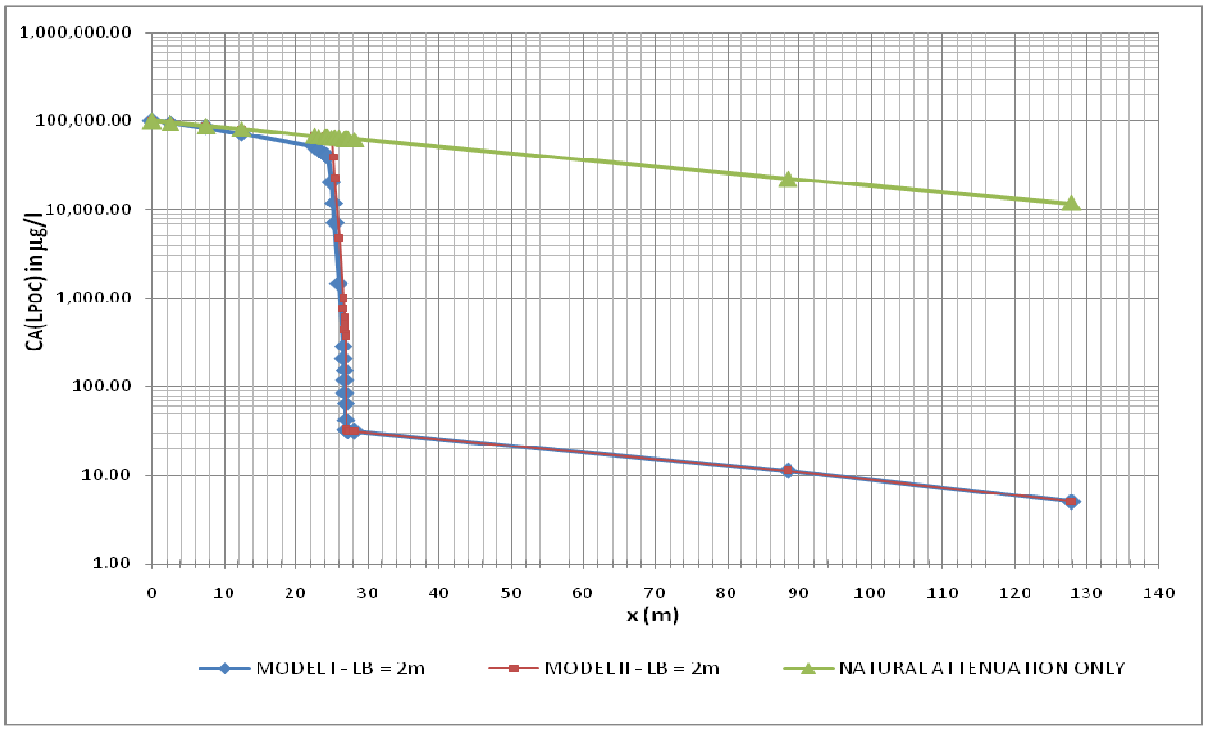

Figure 2-2 b: Contaminant concentrations calculations using Solution I and Solution II - Example (b)-

The contaminant concentrations given by Solution I and Solution II are very comparable. Due to the scale of the figures, these concentrations seem to be almost identical however they are slightly different. The highest percentage of difference encountered between the calculated concentrations given by the two solutions was approximately 0.2 percent for example (a) and approximately 8.2 percent for example (b). These examples reflect the typical feel of how both models compare. This important result suggests that Solution II is a good substitute for the more complex Solution I.

2.5.2 Sensitivity to the distance to the PRB (L_A) from the contaminant source area

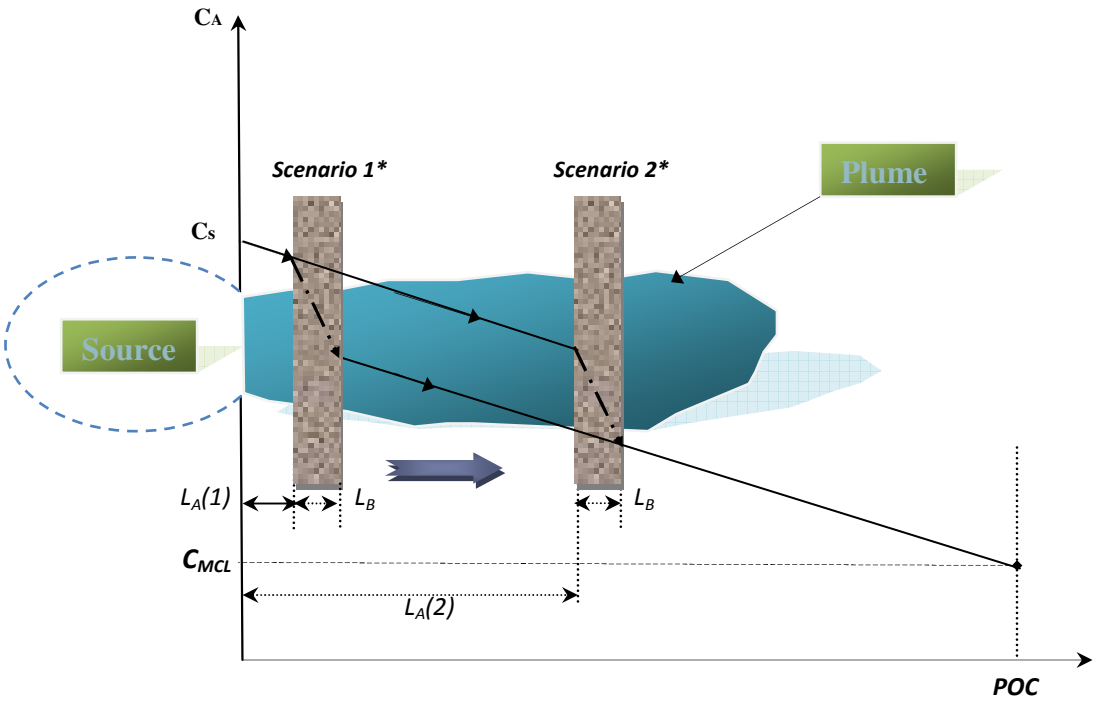

Figure 2- 3: Scenarios of a PRB placed at two different distances from the source of contamination.

Scenario 1 when the PRB is placed at a distance $L_A(1)$ from the source of the contaminant.

Scenario 2 when the PRB is placed at a distance $L_A(2)$ from the source of the contaminant.

Figure 2-3 suggests that a PRB placed at a distance $L_A(1)$ downgradient from the source of contaminant will achieve the same goal of degrading the contaminant to a maximum contaminant level C_{MCL} at a Point of compliance POC as if the PRB was placed at a different distance $L_A(2)$ from the source of contaminant. The PRB will most likely have to be longer if placed away from the source area to account for the expected expansion of the plume downgradient resulting in a possible increase in the construction costs

The one-dimensional Solution I was applied to two hypothetical examples (c) and (d) randomly picked to support the latter assumption. Three scenarios were considered:

1. When the PRB is placed immediately downgradient from the source of contaminant where the distance L_A is chosen as $2m$

2. When the PRB is placed halfway between the source of contaminant and the POC where the distance L_A is chosen as $40m$

3. When the PRB is placed just 10m for example (c) and $50m$ away from the POC where the distance L_A is chosen as $90m$

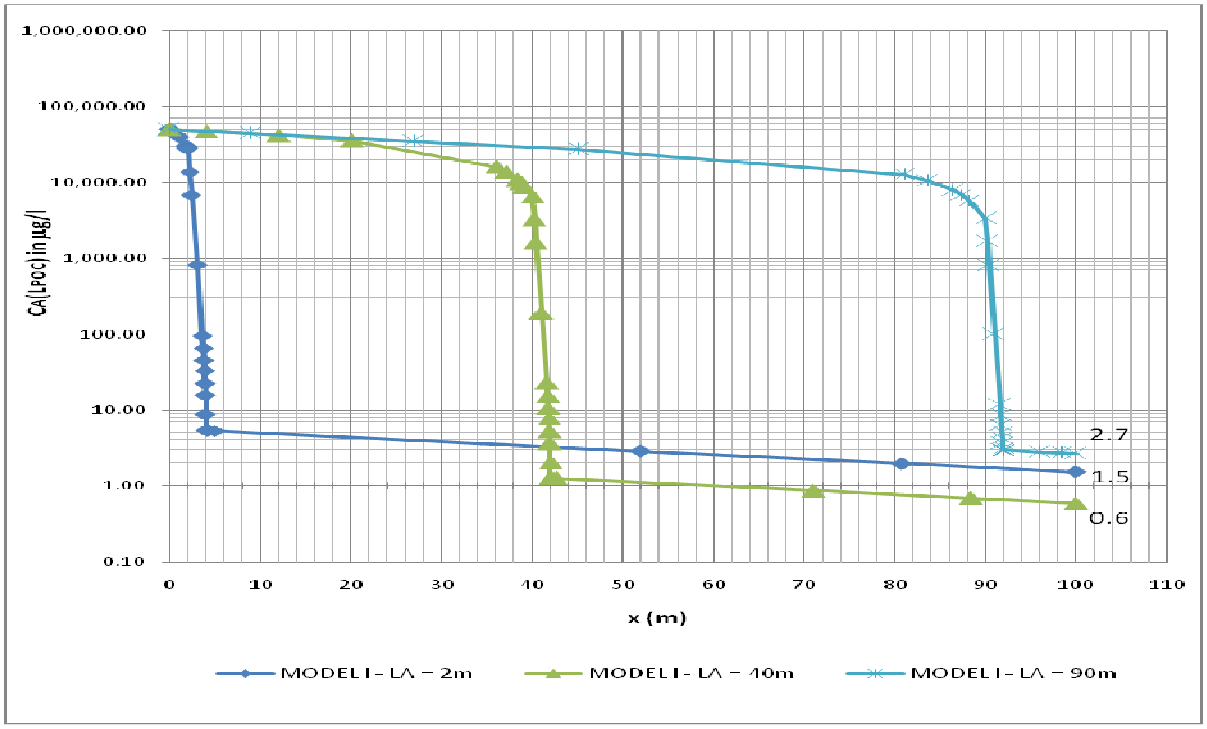

Figure 2-4- a : Contaminant concentrations calculations with 3 different values of L_A

- Example (c)-

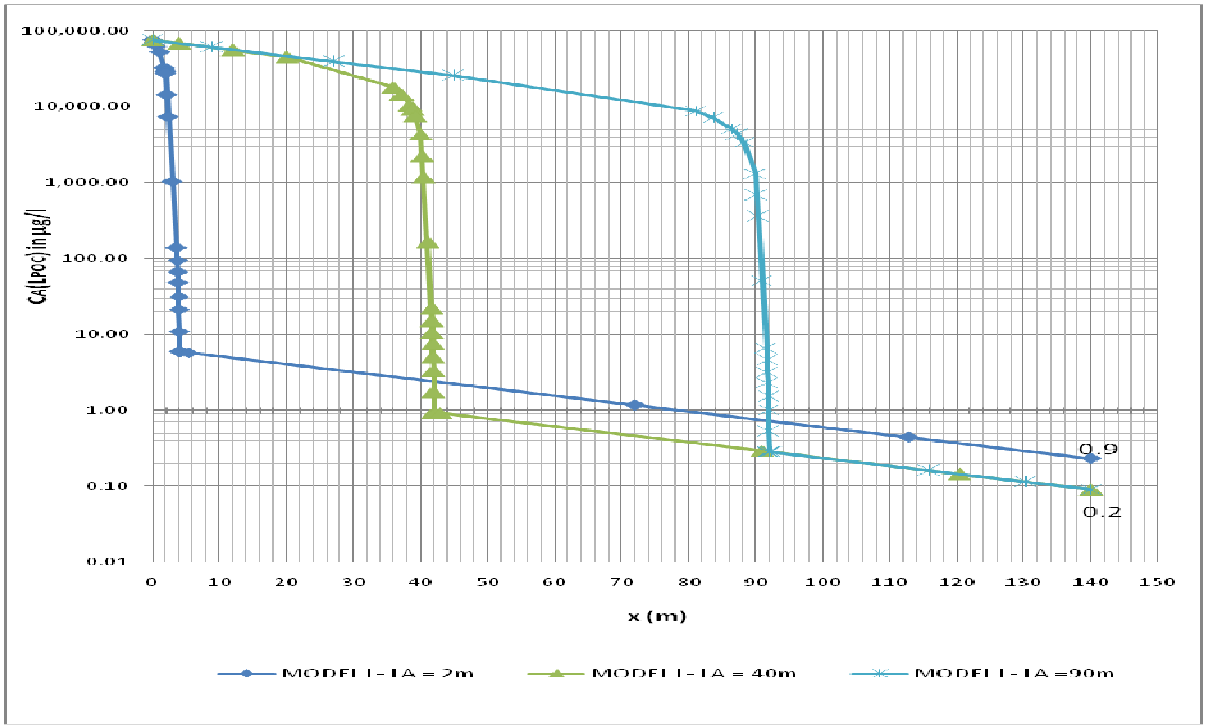

Figure 2-4- b : Contaminant concentrations calculations with 3 different values of L_A

- Example (d)-

The results illustrated in Figure 2-4a and Figure 2-4b indicate that the PRB will have the same performance no matter how far from the source of contaminant it is placed as long as it is in the flowpath of the contaminant plume

2.5.3 Sensitivity to the thickness of the PRB (L_B)

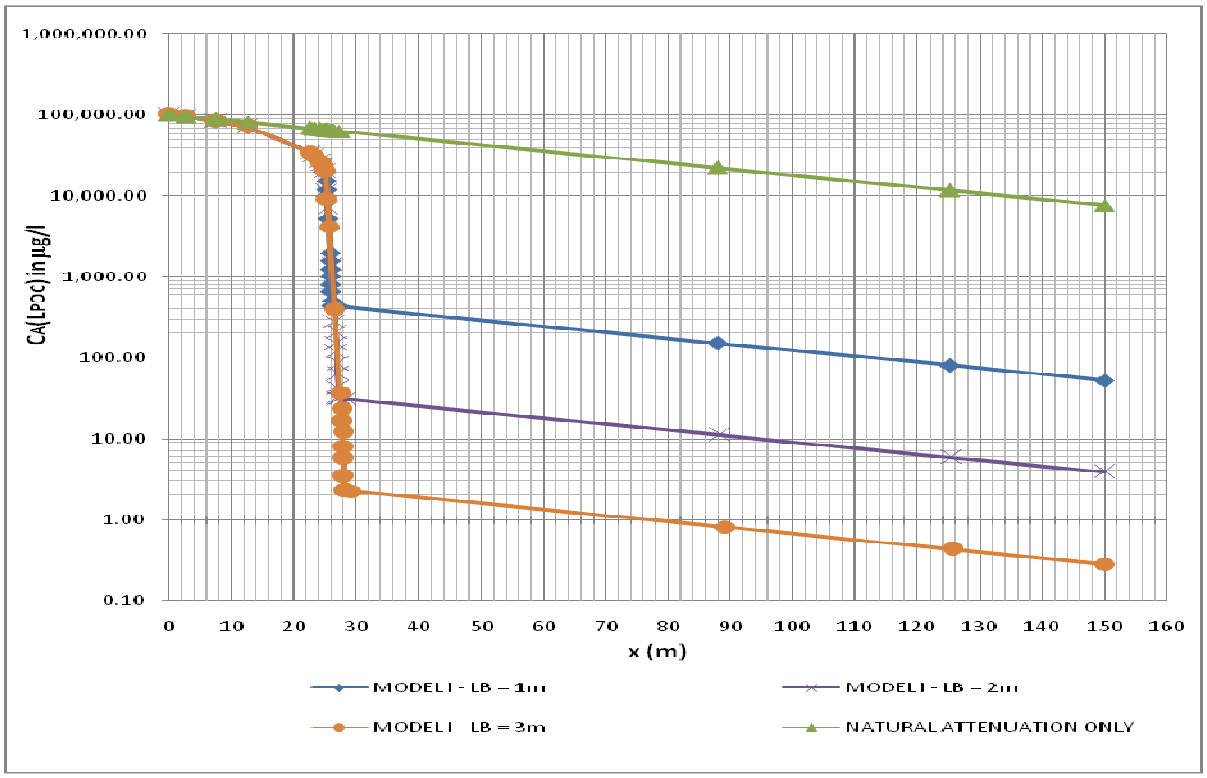

Figure 2-5-a: Concentrations of a Contaminant calculated upgradient, downgradient and within a PRB system using solutions of Model I and Model II, for different PRB thicknesses.

-Example (e)-

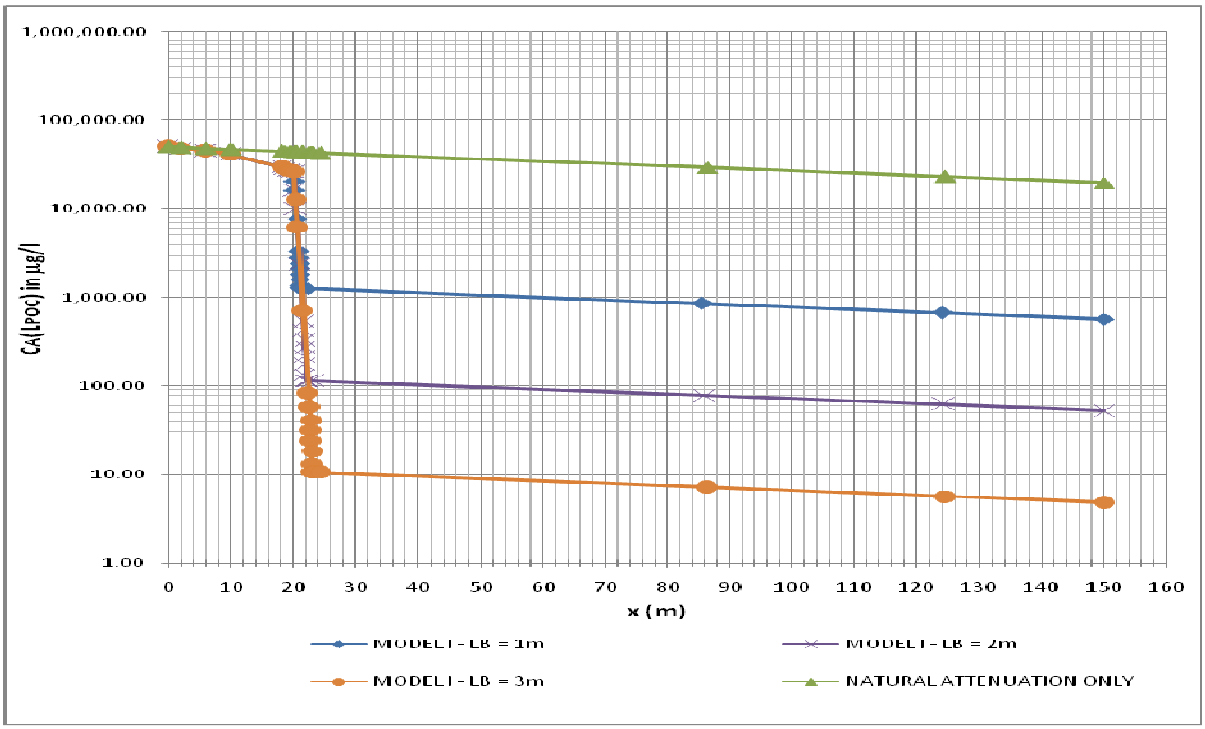

Figure 2-5-b: of Concentrations of a Contaminant calculated upgradient, downgradient and within a PRB system using solutions of Model I and Model II, for different PRB thicknesses.

-Example (f)-

Solution I was used to calculate contaminant concentrations in different locations along the flowpath of a contaminant traveling through a PRB using two randomly picked hypothetical examples (e) and (f). The results of this analysis are shown in Figures 2-5-a and 2-5-b, together with the concentration profiles in the aquifer without PRB when only Natural attenuation is degrading the contaminant.

As expected, both examples show that the thicker the PRB is the faster the degradation of the contaminant will be.

2.5.4 Sensitivity to NAC inside PRB

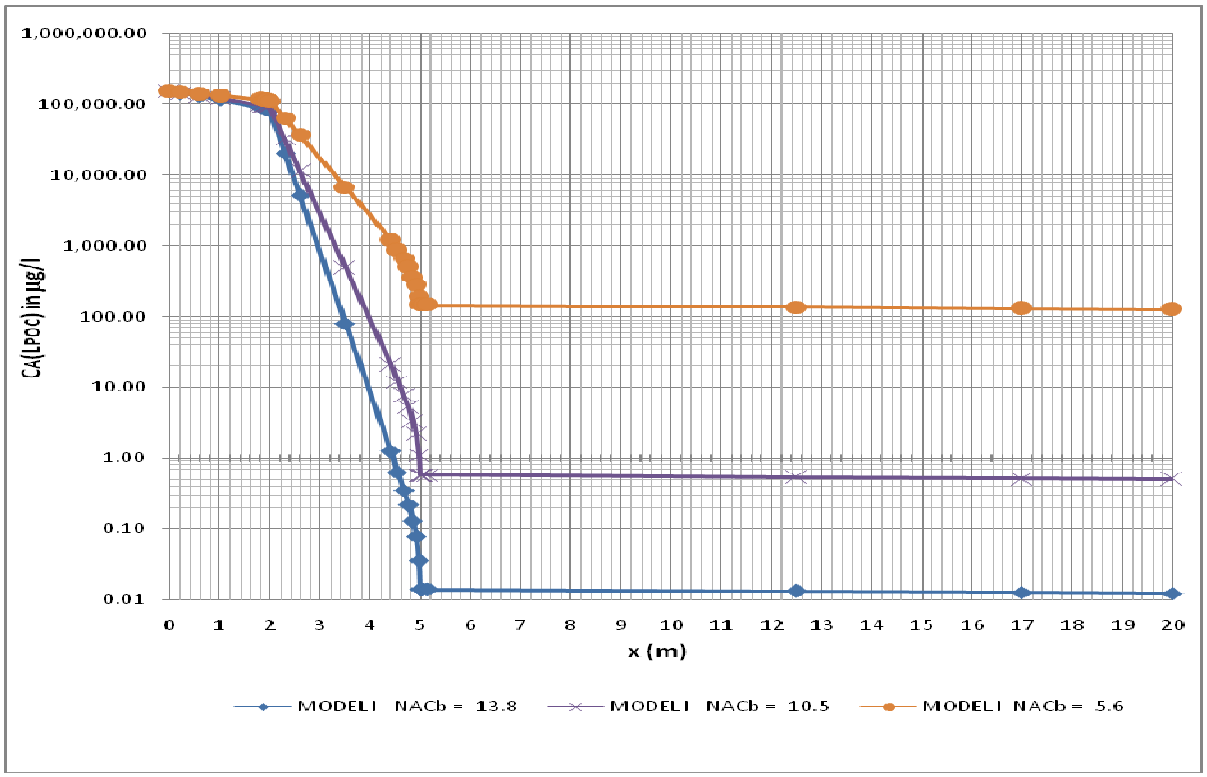

Figure 2- 6: Concentrations of a Contaminant calculated upgradient, downgradient and within a PRB system using solutions of Model I, for different NAC_B^{nd} values

-Example (g) –

Solution I was used to calculate contaminant concentrations in different locations along the flowpath of a contaminant traveling through a PRB using a randomly picked hypothetical example (g). By keeping all of the example's parameters of the aquifer the same and varying the parameters L_B v_B and λ_B of its PRB, the reactive capacity NAC_B^{nd} varied between -13.8, -10.5 and -5.6. The results of this analysis are shown in Figure 2-6, together with the concentration profiles in the aquifer without PRB when only Natural attenuation is degrading the contaminant.

As expected, the lower the PRB reactive capacity NAC_B^{nd}, the faster the contaminant degrades. Also, Figure 2-6 shows that once the contaminant leaves the PRB it degrades with the same natural attenuation capacity of the aquifer NAC_A^{nd} for all three scenarios.

Chapter 3

Design Methodology

3.1 Design Methodology I

3.1.1 Fundamental components of model I

When a PRB with a thickness L_B is placed perpendicular to the path of the contaminant plume at a distance L_A from a source of a contaminant, the contaminant concentration is function of many fundamental components imposed by the receiving aquifer and the reactive material constituting the PRB. Twelve fundamental components were considered in this study to develop a methodology to design PRBs given their contaminant remediation targets.

The contaminant concentration at a POC can be described as a function of variables as shown below:

$$C_A(x = L_{POC}) = f(D_A, D_B, V_A, V_B, \lambda_A, \lambda_B, L_A, L_B, n_A, n_B, C_s, L_{POC}) \quad \text{.....(3-1)}$$

$$V_A n_A = V_B n_B \quad \text{.....(3-2)}$$

where,

D_A : Aquifer hydrodynamic dispersion coefficient [L^2/T].

D_B : Barrier molecular diffusion coefficient [L^2/T].

V_A : Flow velocity in the aquifer [L/T].

V_B : The water velocity in the reactive barrier [L/T].

λ_A : Aquifer biodegradation decay rate [T^{-1}].

λ_B : First-order decay rate inside the reactive barrier [T^{-1}].

L_A : Distance to the reactive barrier from source [L].

L_B Thickness of the reactive barrier [L].

L_{POC} : Distance to the point of compliance from the source [L].

n_A : Effective porosity of the aquifer [L^3/L^3].

n_B : Effective porosity of the reactive barrier [L^3/L^3].

C_s : Initial source concentration [M/L^3].

3.1.1.1 Aquifer hydrodynamic dispersion coefficient (DA)

The aquifer hydrodynamic dispersion coefficient D_A can be determined from the flow velocity in the aquifer (V_A) and the aquifer biodegradation decay rate (λ_A). Assuming that:

$$D_A = \alpha_L V_A \quad \text{.....(3-3)}$$

α_L is the dispersivity which can be estimated by Xu and Epstein (1995) formula.

$$\alpha_L = 0.83 (\log(L_P))^{2.414} \quad \text{.....(3-4)}$$

where L_P is the plume length (m). Assuming that the logarithm of the concentration varies linearly with distance, with the natural attenuation capacity (NAC) as the slope (i.e., $\ln(C_A) = \ln(C_s) - NAC_A X$ **),** with $NAC_A = \dfrac{-V_A + \sqrt{V_A^2 + 4D_A\lambda_A}}{2D_A}$

Therefore, $\ln(PCL) = \ln(C_s) - NAC_A L_P$ where PCL is a very small value (e.g., $2\mu g/l$).

Thus

$$L_P = \frac{\ln(C_s/2)}{NAC_A} \qquad \text{.....(3-5)}$$

Since $D_A = \alpha_L V_A$ therefore using 2-34 and 2-35:

$$D_A = 0.83\left(\log\left(\frac{\ln(C_s/2)}{\dfrac{-V_A + \sqrt{V_A^2 + 4D_A\lambda_A}}{2D_A}}\right)\right)^{2.414} V_A \qquad \text{.....(3-6)}$$

$$f(D_A) = D_A - 0.83\left(\log\left(\frac{\ln(C_s/2)}{\dfrac{-V_A + \sqrt{V_A^2 + 4D_A\lambda_A}}{2D_A}}\right)\right)^{2.414} V_A \qquad \text{.....(3-7)}$$

where D_A is the zero of the function *f* of the Equation (3-7).

3.1.1.2 Simplified Model I

As suggested in section 2.5.2, the contaminant concentration calculated at a *POC* is insensitive to the location of the PRB so the parameter L_A is omitted from Equation 3-1. As a direct

conclusion from section 3.1.1.1 and Equation 3-2 the contaminant concentration at POC for a PRB system is simplified to the following model:

$$C_A(x = L_{POC}) = f(V_A, V_B, \lambda_A, \lambda_B, L_B, C_s, L_{POC}) \quad \text{.....(3-7)}$$

where

V_A : Flow velocity in the aquifer [L/T].

V_B : The water velocity in the reactive barrier [L/T].

λ_A : Aquifer biodegradation decay rate [T^{-1}].

λ_B : First-order decay rate inside the reactive barrier [T^{-1}].

L_B : Thickness of the reactive barrier [L].

L_{POC} : Distance to the point of compliance from the source [L].

C_s : Initial source concentration [M/L^3].

3.1.2 Standard curves

Using Solution I and the database of the 7,500 hypothetical cases developed for this study, $\frac{C_A(x = L_{POC}, V_A, \lambda_A)}{C_s}$ ratios that correspond to the concentrations of contaminant calculated at POC divided by the concentrations of contaminant at source were calculated for all the hypothetical cases. These ratios were found to be increasing when increasing Dk_{wall} . Dk_{wall} vs. $\frac{C_A(x = L_{POC}, V_A, \lambda_A)}{C_s}$ curves were fitted to power functions with very high confidence levels (>89%) (Figure 3-1).

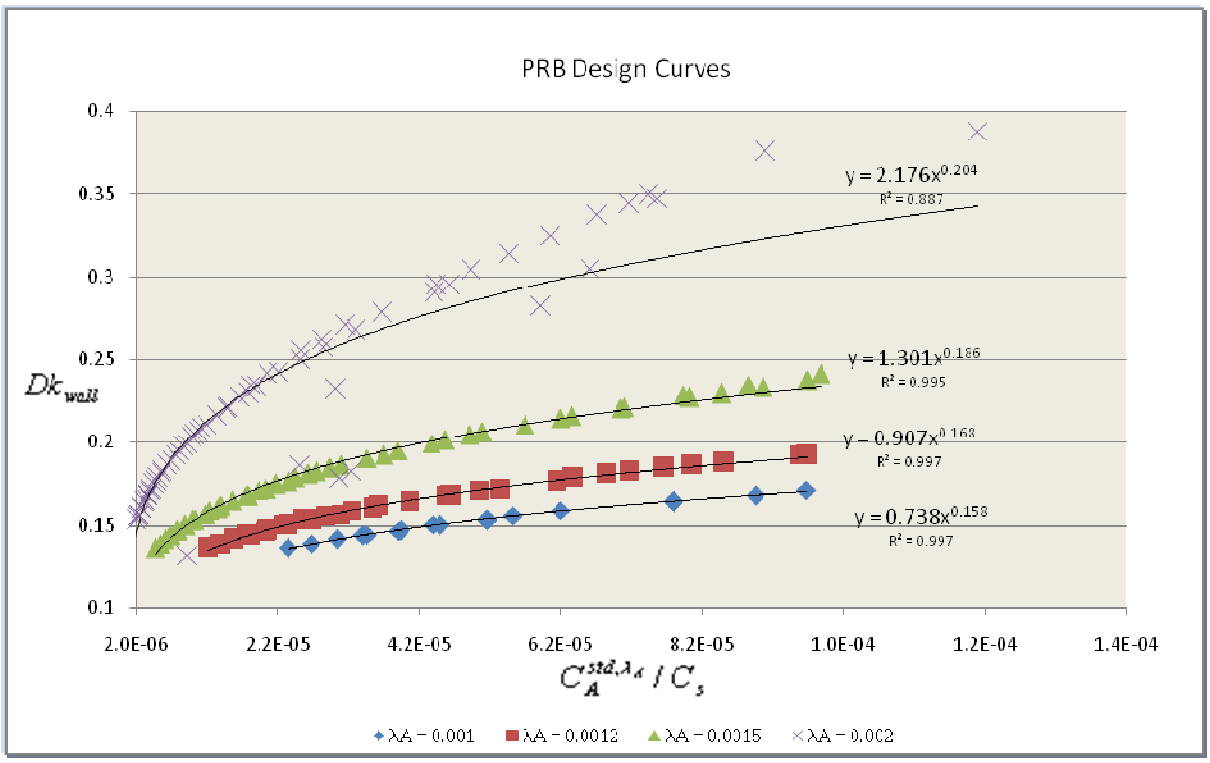

Figure 3- 1 : PRB Design Curves Dk_{wall} *vs.* $C_A^{std,\lambda_A}/C_s$

In this study, standard curves Dk_{wall} *vs.* $C_A^{std,\lambda_A}/C_s$ were defined as Dk_{wall} vs. $\frac{C_A(x=L_{POC},V_A,\lambda_A)}{C_s}$ curves when L_{POC} is equal to $400m$ and V_A is equal to $0.1m/d$

3.1.3 Steps to the empirical design equation I

As a result of Figure 3-1 Dk_{wall} can be written as:

$$Dk_{wall}=\Phi_{\lambda_A}*\left(\frac{C_A^{std,\lambda_A}}{C_s}\right)^{\Psi_{\lambda A}} \qquad \text{.....(3-8)}$$

where Φ_{λ_A} and Ψ_{λ_A} functions that depend on the decay aquifer λ_A. These parameters were

fitted to curves as follows:

$$\Phi_{\lambda_A} = 0.248 * e^{1088\,\lambda_A} \qquad \text{.....(3-9)}$$

$$\Psi_{\lambda_A} = 46.34 * \lambda_A + 0.113 \qquad \text{.....(3-10)}$$

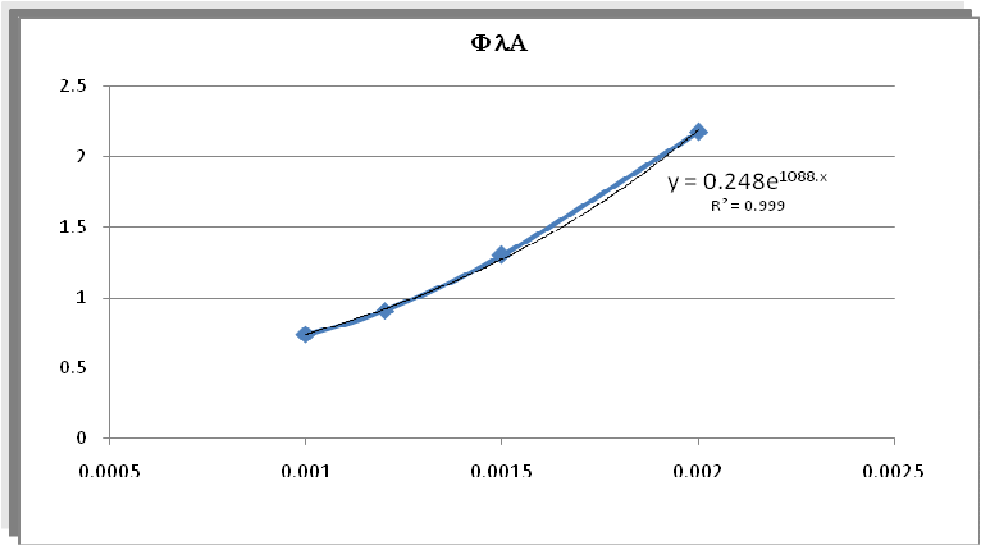

Figure 3- 2 : Dimensionless Correction Factor Φ_{λ_A}

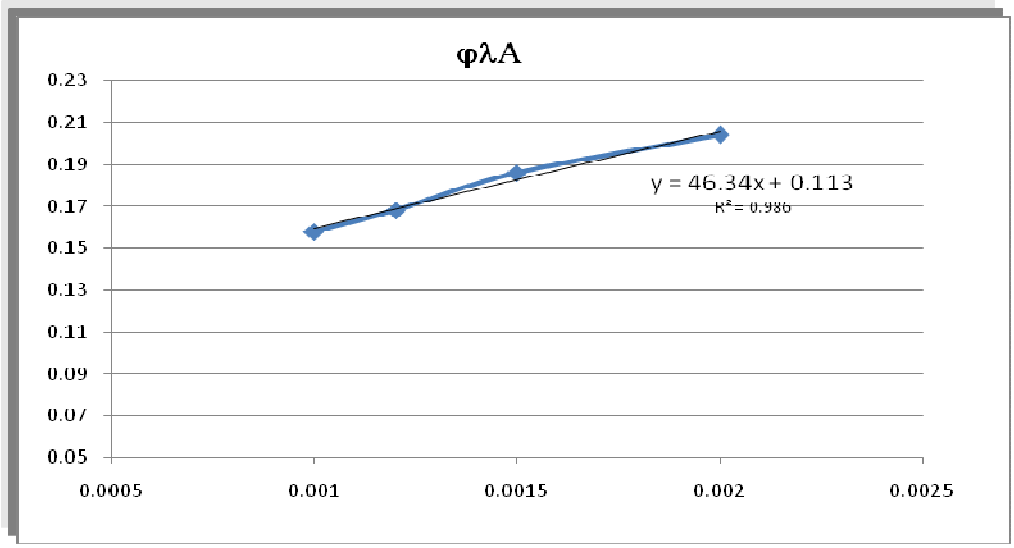

Figure 3- 3 : Dimensionless Correction Factor Ψ_{λ_A}

$C_A\left(L_{POC}, V_A, \lambda_A = 0.001d^{-1}\right)$ by $C_A\left(L_{POC} = 400m, V_A, \lambda_A = 0.001d^{-1}\right)$ ratios were calculated (see Table 3-1). The velocity of the aquifer V_A varies from a minimum of $0.02m/d$ to a maximum of $1m/d$, the distance L_{POC} varies from a minimum of $25m$ to a maximum of $1000m$, and the aquifer biodegradation decay rate λ_A is equal to $0.001d^{-1}$.

Then, $\ln\left(\frac{C_A\left(L_{POC}, V_A = 0.1m/d, \lambda_A = 0.001d^{-1}\right)}{C_A^{std}}\right)$ by $\ln\left(\frac{C_A\left(L_{POC}, V_A, \lambda_A = 0.001d^{-1}\right)}{C_A\left(L_{POC} = 400m, V_A, \lambda_A = 0.001d^{-1}\right)}\right)$ ratios were calculated (see Table 3-2). It was found that these ratios depend on the velocity of the aquifer only.

Table 3- 1: $\frac{C_A\left(L_{POC}, V_A, \lambda_A = 0.001d^{-1}\right)}{C_A\left(L_{POC} = 400m, V_A, \lambda_A = 0.001d^{-1}\right)}$

VA (m/d)	POC (m)					
	25	**75**	**200**	**600**	**800**	**1000**
0.02	2301648	326412.9892	2472.2302	0.000396	-	-
0.04	2423.875	857.5157865	63.836942	0.015665	0.000245	3.84E-06
0.07	106.6545	57.22449282	12.06671	0.082873	0.006868	0.000569
0.1	29.07649	18.55252402	6.0333109	0.165746	0.027472	0.004553
0.2	5.777388	4.572643322	2.5483368	0.392413	0.153988	0.060427
0.6	1.830086	1.688399715	1.3803359	0.724461	0.524844	0.380229
0.8	1.577078	1.484133067	1.2750339	0.784293	0.615115	0.482431
1	1.441832	1.373175319	1.2154993	0.822708	0.676848	0.556849

Table 3- 2: $\ln\left(\frac{C_A\left(L_{POC}, V_A = 0.1m/d, \lambda_A = 0.001d^{-1}\right)}{C_A^{std}}\right) \Big/ \ln\left(\frac{C_A\left(L_{POC}, V_A, \lambda_A = 0.001d^{-1}\right)}{C_A\left(L_{POC} = 400m, V_A, \lambda_A = 0.001d^{-1}\right)}\right)$

VA (m/d)	POC (m)					
	25	75	200	600	800	1000
0.02	0.230043	0.230042891	0.2300428	0.229392	0.229392	0.229392
0.04	0.432424	0.43242356	0.4324236	0.432424	0.432423	0.432422
0.07	0.721675	0.721675027	0.7216751	0.721675	0.721675	0.721675
0.1	1	1	1	1	1	1
0.2	1.921336	1.921335624	1.9213356	1.921336	1.921336	1.921336
0.6	5.576004	5.576003942	5.5760035	5.576005	5.576004	5.576003
0.8	7.397108	7.397107277	7.3971074	7.397109	7.397108	7.397106
1	9.209606	9.209612596	9.2095838	9.209656	9.209622	9.209636

From Table 3, A_{VA} is a function of the velocity of the aquifer so that:

$$\ln\left(\frac{C_A\left(L_{POC}, V_A = 0.1m/d, \lambda_A = 0.001d^{-1}\right)}{C_A^{std}}\right) \Big/ \ln\left(\frac{C_A\left(L_{POC}, V_A, \lambda_A = 0.001d^{-1}\right)}{C_A\left(L_{POC} = 400m, V_A, \lambda_A = 0.001d^{-1}\right)}\right) = A_{VA} \quad \ldots$$

……..(3-11)

Additionally, when $V_A = 0.1m/d$ (see Table 3-1), B_{POC} is a function of the point of compliance such that:

$$\frac{C_A\left(L_{POC}, V_A = 0.1m/d, \lambda_A = 0.001d^{-1}\right)}{C_A^{std}} = \exp(B_{POC}) \qquad \text{……..(3-12)}$$

Consequently, from (3-11) and (3-12):

$$B_{POC} = A_{VA} * \ln\left(\frac{C_A\left(L_{POC}, V_A, \lambda_A = 0.001d^{-1}\right)}{C_A\left(L_{POC} = 400m, V_A, \lambda_A = 0.001d^{-1}\right)}\right)$$

$$\frac{C_A\left(L_{POC}, V_A, \lambda_A = 0.001d^{-1}\right)}{C_A\left(L_{POC} = 400m, V_A, \lambda_A = 0.001d^{-1}\right)} = \exp\left(\frac{B_{POC}}{A_{VA}}\right)$$

$$C_A(L_{POC}, V_A, \lambda_A = 0.001d^{-1}) = C_A\left(L_{POC} = 400m, V_A, \lambda_A = 0.001d^{-1}\right) * \exp\left(\frac{B_{POC}}{A_{VA}}\right) \quad \text{.....(3-13)}$$

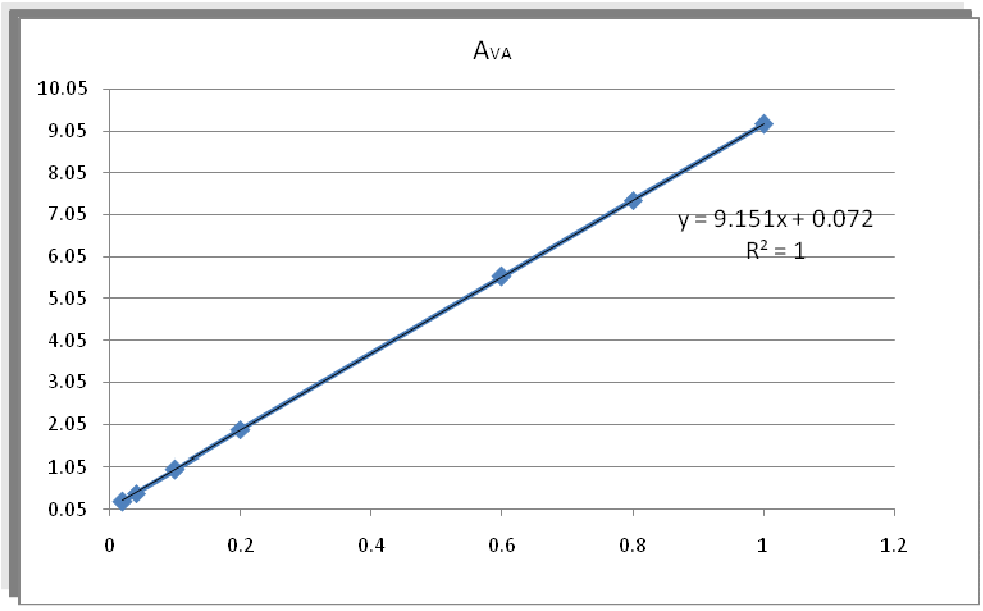

Figure 3- 4: Parameter A_{VA}

$$A_{VA} = 9.151 * V_A + 0.072 \quad \text{.....(3-14)}$$

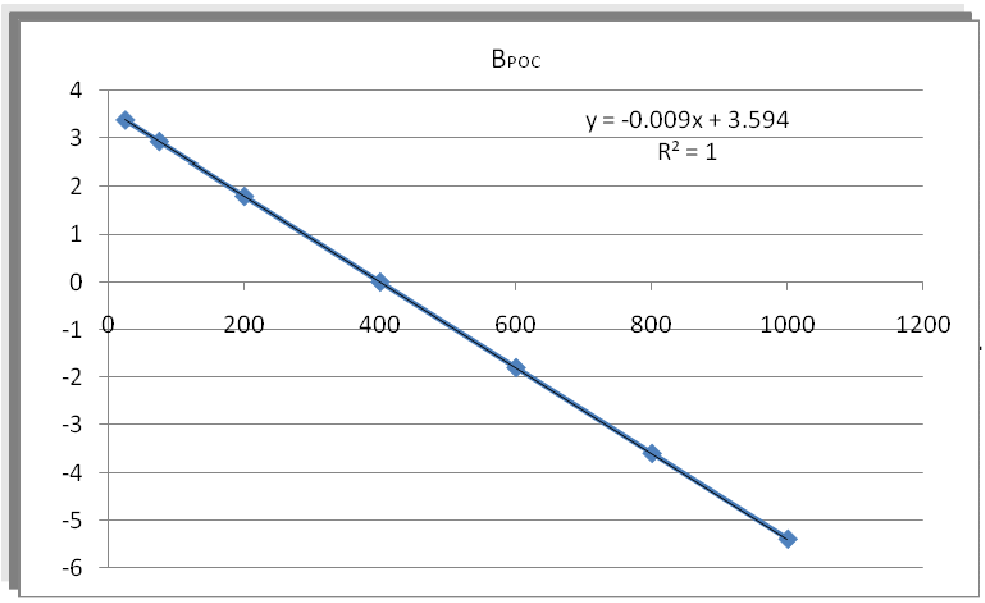

Figure 3- 5: Parameter B_{POC}

$$B_{POC} = -0.009 * L_{POC} + 3.594 \quad \text{.....(3-15)}$$

$C_A\left(L_{POC} = 400m, V_A, \lambda_A = 0.001d^{-1}\right)$ by C_A^{std} ratios were then calculated for different velocities of aquifer V_A .(see Table 3-3)

Table 3- 3: $\frac{C_A\left(L_{POC} = 400m, V_A, \lambda_A = 0.001d^{-1}\right)}{C_A^{std}}$ **vs.** V_A

V_A (m/d)	$\frac{C_A\left(L_{POC} = 400m, V_A, \lambda_A = 0.001d^{-1}\right)}{C_A^{std}}$
0.02	7.85296E-06
0.04	0.009319187
0.06	0.118268274
0.08	0.443341395
0.1	1

V_A (m/d)	$\frac{C_A\left(L_{POC}=400m, V_A, \lambda_A=0.001d^{-1}\right)}{C_A^{std}}$
0.2	5.398266307
0.3	9.685354635
0.6	17.64225402
0.8	20.55409107
1	22.54114178

From the Table above,

$$\frac{C_A\left(L_{POC}=400m, V_A, \lambda_A=0.001d^{-1}\right)}{C_A^{std}} = D_{VA} \qquad \text{.....(3-16)}$$

where:

$$\begin{cases} D_{VA} = 279.82 * V_A^2 - 22.69 * V_A + 0.47 & \text{when} \quad 0.04 \le V_A \le 0.1 \\ D_{VA} = -23.7 * V_A^2 + 49.5 * V_A - 3.7 & \text{when} \quad 0.1 \le V_A \le 1 \end{cases} \qquad \text{.....(3-17)}$$

Finally, all the previous steps that generated Tables 2, 3 and 4 were repeated for aquifer biodegradation decay rate λ_A values varying between $0.0012d^{-1}, 0.0015d^{-1}, 0.0017d^{-1}$, $0.002d^{-1}$, and $0.0025d^{-1}$ to set up a general equation such that:

Using Equations 3-13 and 3-16:

$$\left(C_A(L_{POC}, V_A, \lambda_A)\right)^{\frac{0.001}{\lambda_A}} = C_A^{std,\lambda_A} * D_{VA} * \left(\exp\left(\frac{B_{POC,\lambda_A}}{A_{VA}}\right)\right)^{\frac{0.001}{\lambda_A}} \qquad \text{.....(3-18)}$$

where:

$$B_{POC,\lambda_A} = -8.588 * \lambda_A * L_{POC} + 3439.5 * \lambda_A + 0.0639 \qquad \text{.....(3-19)}$$

3.1.4 Empirical Design Methodology I

From Equations 3-8 and 3-18 we can calculate the design Dk_{wall} needed to degrade the contaminant to C_{MCL}. The design thickness of a PRB L_B, which corresponds to the thickness of a PRB that reduces the contaminant to C_{MCL} at a given distance to the POC, is calculated as follows:

$$L_B = \frac{V_B}{Dk_{wall} * \lambda_B} \qquad \text{.....(3-20)}$$

where

$$Dk_{wall} = 0.248 * \exp(1088\lambda_A) * \left(\frac{1}{D_{VA} * C_S} * \left(\frac{C_{MCL}}{\exp\left(\frac{B_{POC,\lambda A}}{A_{VA}} \right)} \right)^{\frac{0.001}{\lambda A}} \right)^{46.34\lambda_A + 0.113} \qquad \text{....(3-21)}$$

3.2 Design Methodology II

Using *Solution II* (section 2.4.2), a simple equation is obtained to calculate the design thickness of a PRB capable of degrading the contaminant to C_{MCL} at a given L_{POC} (See Appendix B):

$$L_B = \frac{\ln\left(\frac{C_s}{C_{MCL}}\right) - NAC_A * L_{POC}}{NAC_B - NAC_A} \qquad \text{.....(3-22)}$$

where NAC_A = natural attenuation capacity in the aquifer= $NAC_A = \frac{-V_A + \sqrt{V_A^2 + 4D_A\lambda_A}}{2D_A}$, and

NAC_B =natural attenuation capacity in the PRB = $NAC_B = \frac{-V_B + \sqrt{V_B^2 + 4D_B\lambda_B}}{2D_B}$

3.3 Model Performance

Using both the empirical and the analytical design equations, the design thicknesses of the PRBs were calculated for all the 7,500 hypothetical examples that were generated for this study, followed by a statistical analysis to verify the performance of each methodology. Figure 3-6 and Figure 3-7 illustrate the number of occurrence by margin of error observed between the calculated design thickness and the real thickness for all the hypothetical examples.

Even though the analytical design equation was derived from the simplified Solution II, this method has shown exceptional results unlike the empirical design equation that introduced a larger incertitude. Indeed, 95 percent of the time, the analytical equation estimated the thickness of the PRB just 15 % lower or higher than its real value versus only approximately 45 percent of the time for the empirical design equation.

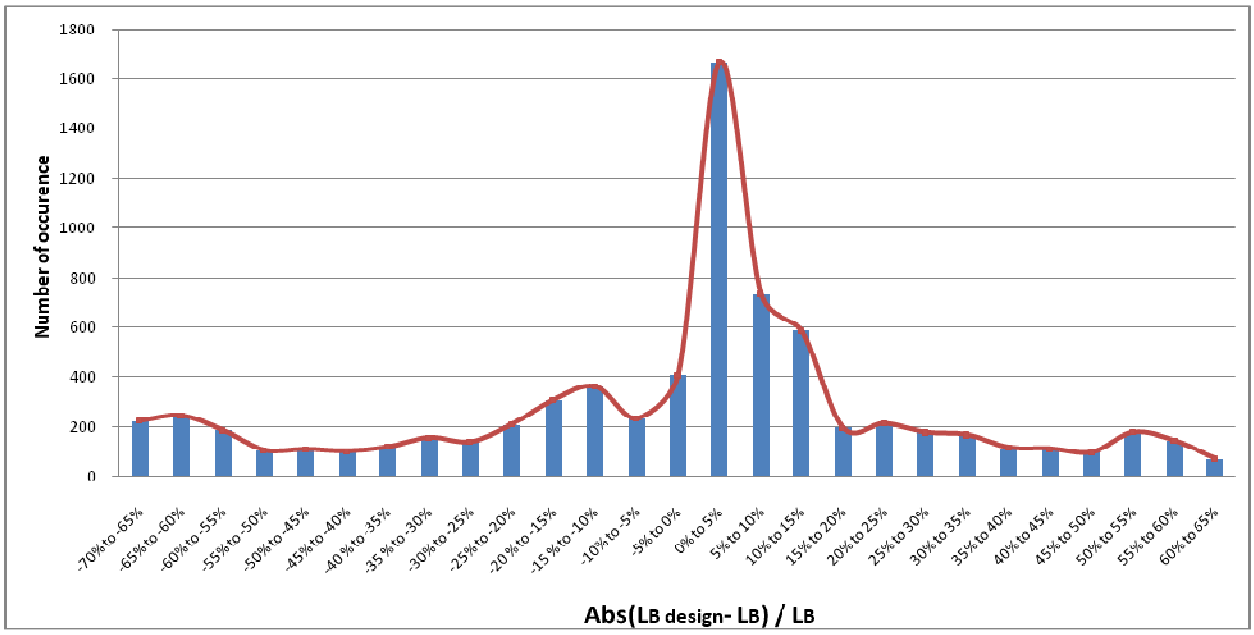

Figure 3- 6: Empirical Design Equation performance

-Model I-

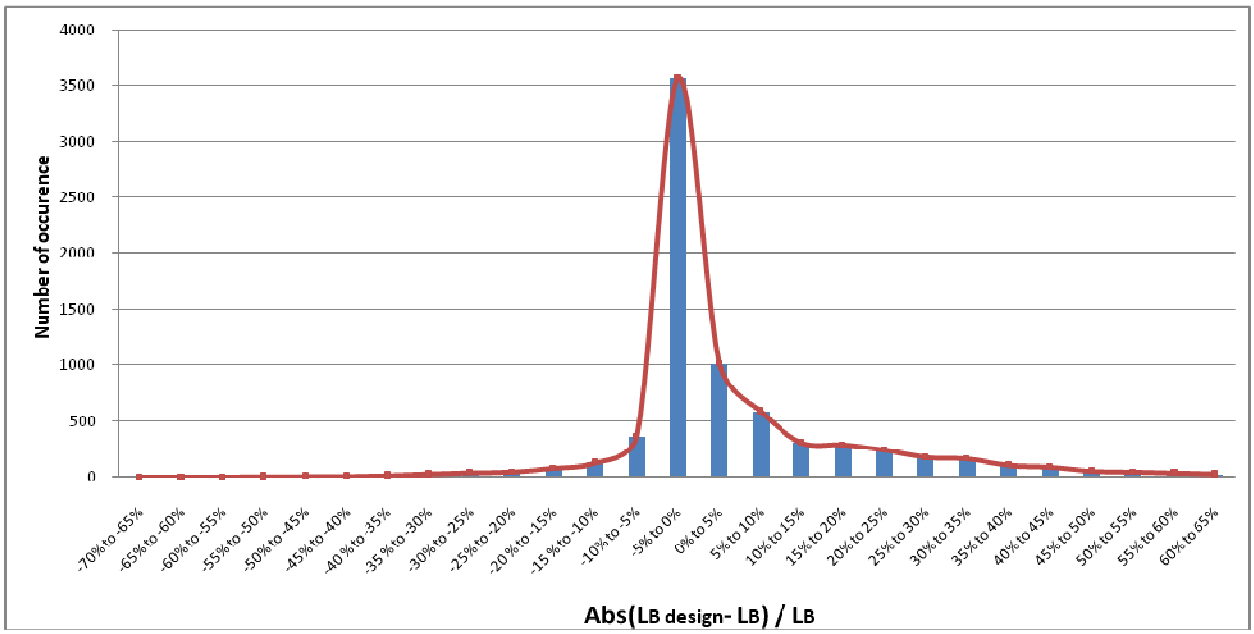

Figure 3- 7: Analytical Design Equation performance

-Model II-

Chapter 4

Case Study

4-1. Problem Background

A pilot-scale PRB filled with zero-valent iron (ZVI) was installed in April 1996 at Moffett Field in Mountain View California (Figure 4-1) to treat a portion of a large groundwater Plume of chlorinated volatile organic compounds (CVOCs) contaminants, primarily trichloroethene (TCE), *cis*-1,2-dichloroethylene (*cis*-1,2-DCE),and perchloroethene (PCE), that is approximately two miles long and 5,000 feet wide (Figure 4-2), oriented North/North-East , with high TCE concentrations that could exceed 5,000 µg/l (Figure 4-3).

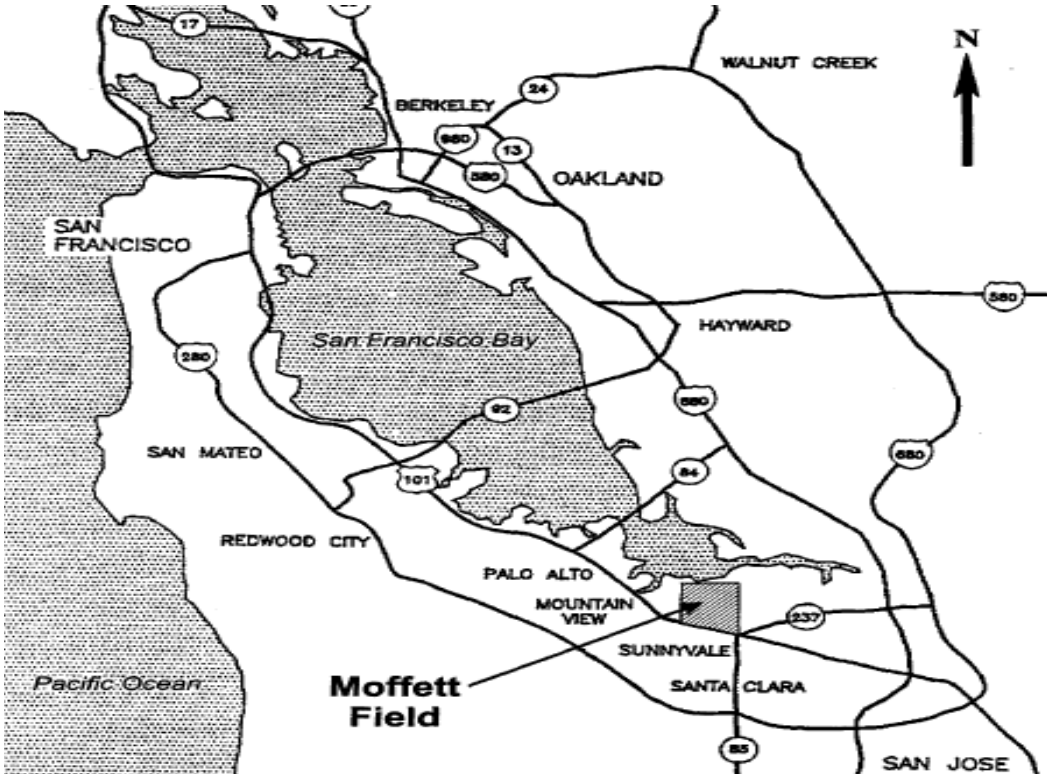

Figure 4- 1: Map of San Francisco and vicinity (Battelle., 1998)

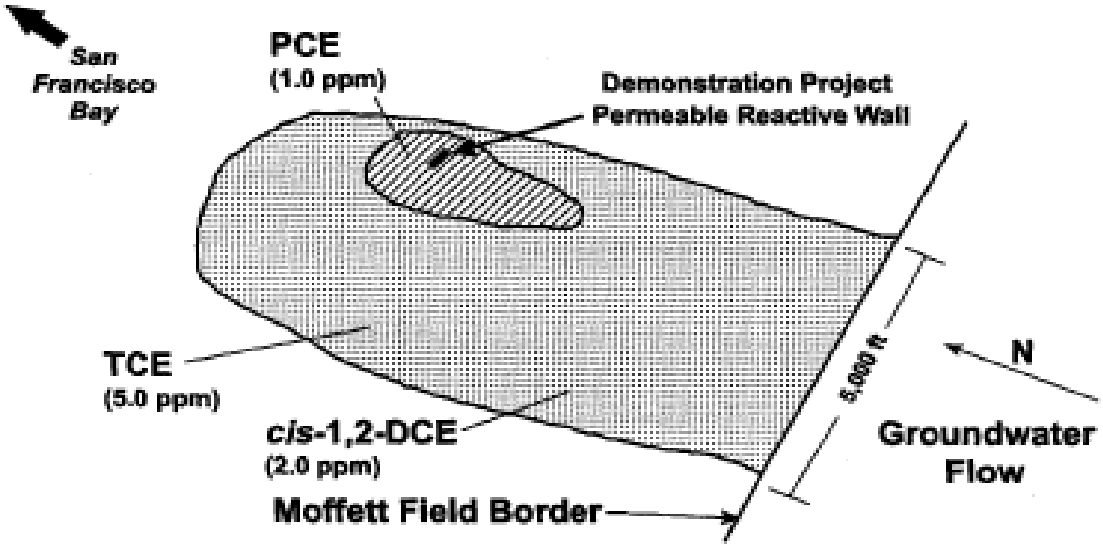

Figure 4- 2 : Moffett Field solvent plume (Battelle., 1998)

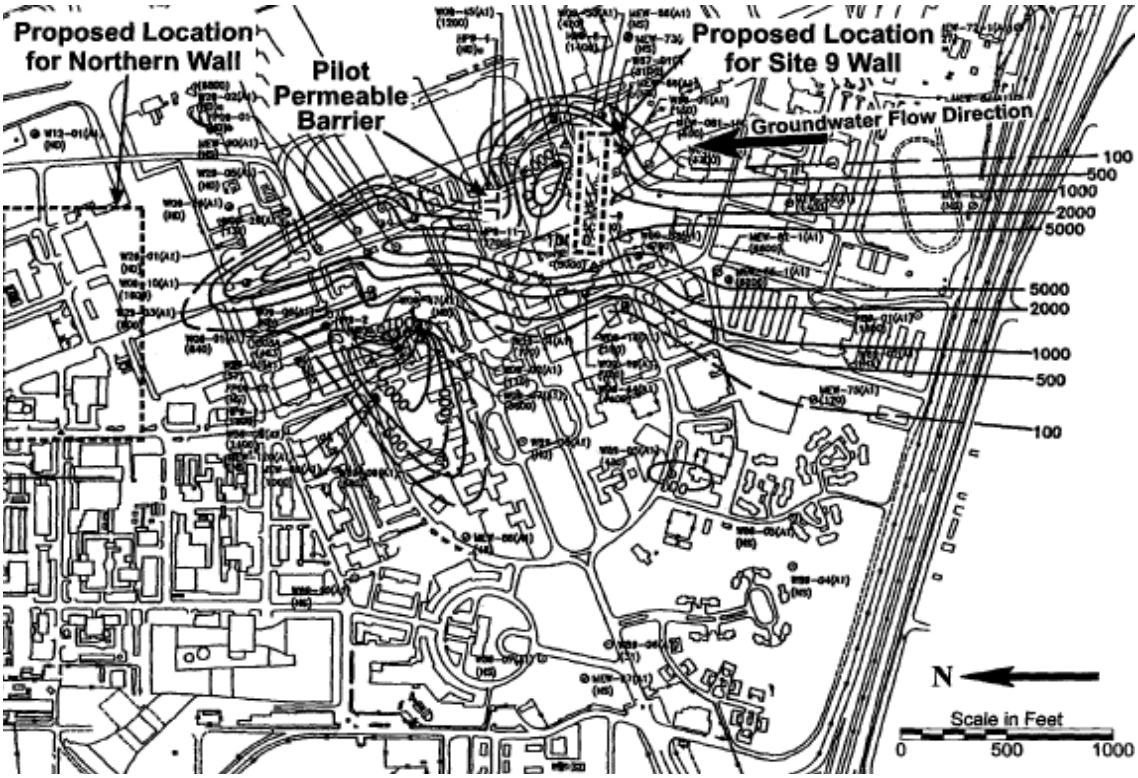

Figure 4- 3 : TCE concentration contour map (IT Corp., 1991)

4-2. Parameter estimation

4-2-1 The natural attenuation capacity in the aquifer NAC_A estimation

Monitoring wells are installed in and around the Moffett Field's pilot-scale PRB at different depths along the flow path (Figure 4-4). Monitoring wells WCI-1 and WCI-3 were retained for this analysis because they are further upgradient and downgradient from the PRB. Additionally, they were sampled in January 1997, only few months after the installation of the PRB. Using the monitoring results for primary target CVOCs (Table 4-1) of January 1997, a total concentration of

$3180 \mu g / l$ was observed at well WIC-1. A total concentration of $3160 \mu g / l$ was observed at well WIC-3. Using figure 4-4, The distance between the wells is estimated to be $28 \, feet$. Assuming that the influence of the PRB is not yet felt in these wells, the natural attenuation capacity in the aquifer NAC_A is estimated at $0.00023 m^{-1}$. However the NAC_A of the aquifer can be better estimated from the concentration contour map (Figure 4-3). Using the data from the map, monitoring well (MEW 85-1) indicates a concentration of $6200 \mu g / l$ and, approximately 2250 feet downgradient from it, monitoring well (W09-10) indicates a concentration of $1600 \mu g / l$ which gives an NAC_A of $0.0006 m^{-1}$.

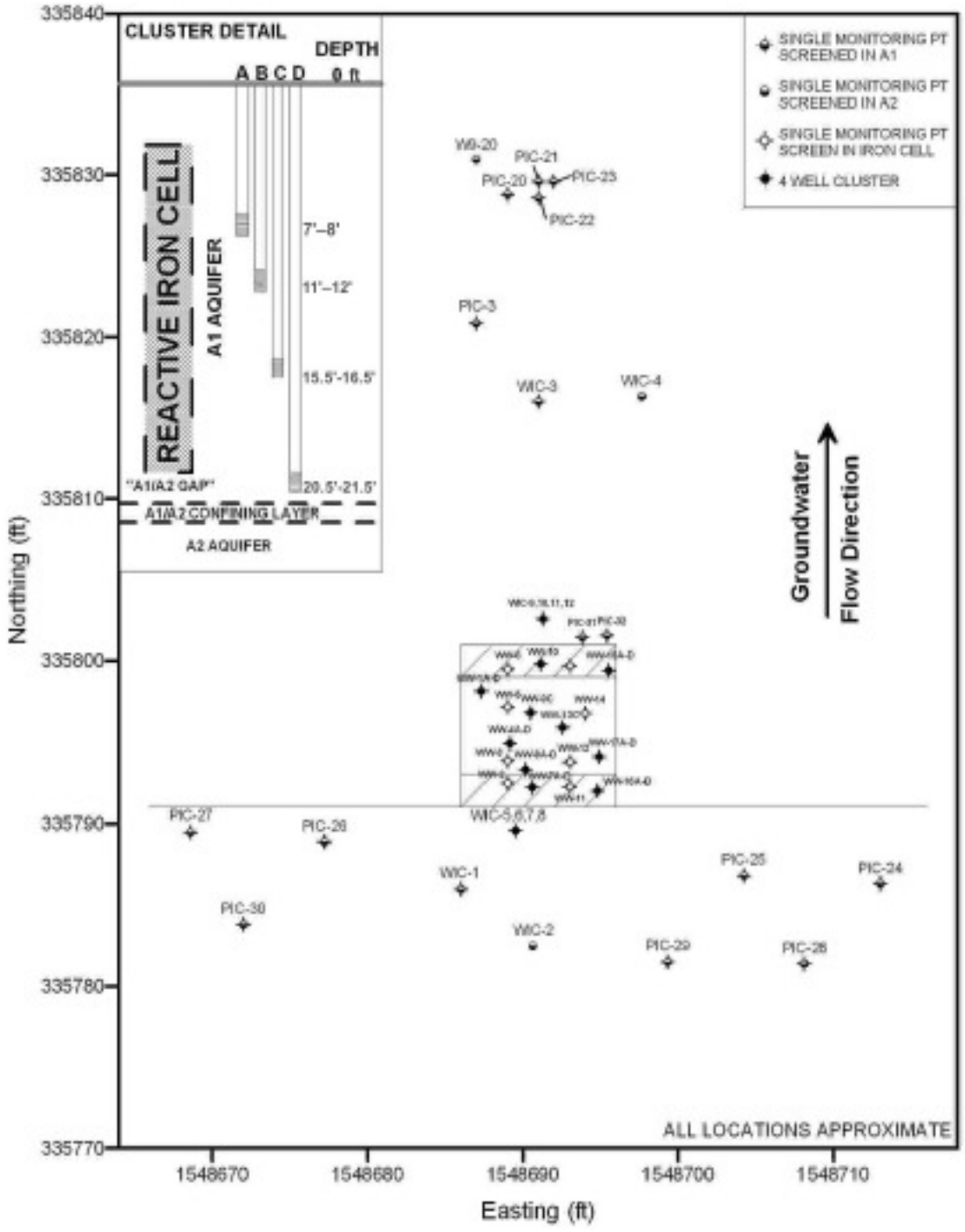

Figure 4- 4: Location of Model Boundaries and Monitoring Wells in the vicinity of the PRB (Battelle., 2005)

4-2-2 First-order decay rate inside the reactive barrier λ_B estimation

A bench-scale study was conducted prior to the installation of the Moffett Field's PRB and its results were used to estimate the first-order rate inside the PRB λ_B (Table 4-2). The projected contaminant half-lives were added up to the vinyl chloride half-life to estimate the first-order rate inside the PRB λ_B that correspond to decaying vinyl chloride using Equation 4-1. For a total half-life of 4.17 hours and the first-order rate inside the PRB λ_B is estimated at approximately $3.99 d^{-1}$.

$$\lambda_B = \frac{\ln(2)}{T_{1/2}} \qquad \text{.....(4-1)}$$

Table 4- 1: Bench-scale Test Results and Design projection (Battelle et al., 1998)

Contaminant	Half-Life in Bench-Scale Test (50:50) Iron-Sand Mixture)	Projected Half-Life For 100% Iron Medium[a]
PCE	0.29 to 0.81 hour	0.13 to 0.35 hour
TCE	0.87 to 1.0 hour	0.38 to 0.43 hour
cis-1,2-DCE	3.1 hours	1.35 hours
Vinyl chloride	4.7 hours	2.04 hours
1,1-DCA	9.9 hours	4.3 hours

(a) Half-lives were reduced by a factor of 2.3 to account for the higher surface area and porosity in 100% iron medium versus in a 50:50 iron-sand (by mass) mixture.

4-2-3 Natural attenuation capacity in the PRB NAC_B estimation

The estimated groundwater velocity in the reactive cell ranges between 0.2 to 2 feet/day, the aquifer porosity n_A is 0.30 and the PRB porosity n_B is 0.33 (Battelle et al., 1998). In order to calculate the maximum PRB thickness needed to remediate the contaminant the maximum velocity of 2 feet/day is used since the faster the groundwater velocity is the ticker the PRB need to be.

When the Barrier molecular diffusion coefficient D_B is equal to $8.60E-05\, m^2/d$ the estimated NAC_B is approximately $7.19 m^{-1}$.

4-2-4 Estimation of LB-design

Using Figure 4-3, approximately 200 feet upgradient from the PRB the concentration of the contaminant is at its maximum. Based on historical data for CVOCs in well W9-35, an aquifer zone well near the current PRB location, the maximum contaminant concentration is approximately $8000 \mu g/l$. This concentration is used in this example as the concentration at source C_s.

The analytical Equation 3.22 calculates the thickness of the PRB that would degrade the contaminant (TCE, PCE, DCE, and vinyl chloride) from the $C_s = 8000 \mu g/l$ to a $C_{MCL} = 2 \mu g/l$ at well WIC-3 approximately 225 feet from source as follows:

$$L_{B-design} = \frac{\ln\left(\frac{8000}{2}\right) - 0.0006 * 225}{7.19 - 0.0006} = 3.7\, feet$$

To allow a 95% confidence on the predicted thickness, a 15 % increase on the calculated design thickness of the PRB was granted. The suggested thickness of the Moffett PRB to degrade all vinyl chloride of the site is $4.3\, feet$ which is lower than actual PRB thickness of 6 feet. This suggests that the PRB will achieve its goals.

Chapter 5

Engineering Significance

The results of this study provide engineers and scientists with a preliminary methodology to design PRBs that can be implemented simply. An empirical design equation and a simple analytical design equation were obtained to calculate the thickness of a PRB capable of degrading a contaminant from a source contaminant concentration C_s to a maximum contaminant level C_{MCL} at a Point of compliance POC. Both equations integrate the fundamental components that drive the natural attenuation process of the aquifer and the reactive capacity of the PRB.

The empirical design equation was derived from a dataset of 7,500 random hypothetical cases that used the solutions of the PRB conceptual model (Solution I). The analytical design equation was derived from particular solutions of the model (Solution II) which the study showed fit the complex solutions of the model well. The study also showed that the analytical design equation performs better. Using the 7,500 hypothetical cases, the analytical equation has shown that it gives an estimated thickness of the PRB just 15 % lower or higher than the real thickness of

the PRB 95 percent of the time. As a conclusion, it is suggested that the thickness be calculated using the analytical design equation and a percentage increase up to 15 percent should be applied so that the estimated thickness will have a high probability of success of up to 95 percent.

To calculate the design thickness of a PRB, Natural attenuation capacity of the aquifer can be estimated from the observed contaminant concentration changes along aquifer flowpaths prior to the installation of a PRB. Bench-scale or pilot testing can provide good estimates of the required residence times (Gavaskar et al. 2000) , which will provide the reactive capacity of the PRB needed for the calculation.

A PRB will better operate when installed perpendicularly to the predominant direction of groundwater flow. The results of this study suggest also that the installation location downgradient from the source of contaminant is flexible. If a PRB is installed in two different locations, it will achieve the same remediation goals. This important finding gives engineers and scientists the choice to adjust the location of their PRBs so that the overall project can be the most feasible and cost effective.

Reference

Gavaskar, A. R., Gupta, N., Sass, B., Fox, T., Janosy, R. J., and Hicks. J. T. "Design guidance for application of permeable reactive barriers for groundwater remediation" Report Prepared for the US-AIR FORCE, Battelle, Columbus, Ohio. 2000

Appendix A

MODEL I

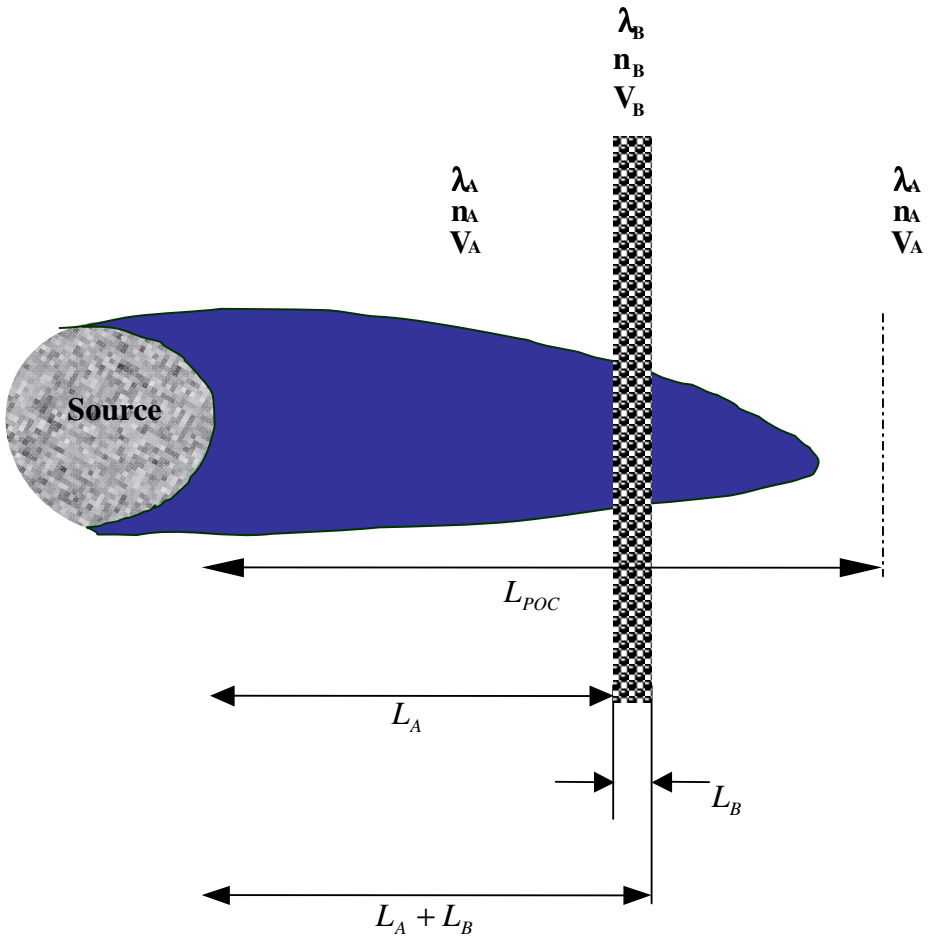

MODEL I

Equations (ODEs, BC, Intermediate conditions)

Governing differential equations

$$0 \le x \le L_A : \qquad D_A \frac{\partial^2 C_1}{\partial x^2} - V_A \frac{\partial C_1}{\partial x} - \lambda_A C_1 = 0 \tag{1}$$

$$L_A \le x \le L_A + L_B : \qquad D_B \frac{\partial^2 C_2}{\partial x^2} - V_B \frac{\partial C_2}{\partial x} - \lambda_B C_2 = 0 \tag{2}$$

$$x \ge L_A + L_B : \qquad D_A \frac{\partial^2 C_3}{\partial x^2} - V_A \frac{\partial C_3}{\partial x} - \lambda_A C_3 = 0 \tag{3}$$

Boundary conditions

$$C_1(x=0) = C_s \tag{4}$$

$$C_3(x) \xrightarrow{x \longrightarrow +\infty} 0 \tag{5}$$

Contact between barrier and aquifer

$$C_1(x = L_A) = C_2(x = L_A) \tag{6}$$

$$C_2(x = L_A + L_B) = C_3(x = L_A + L_B) \tag{7}$$

$$-D_B n_B \frac{\partial C_2}{\partial x} + V_B n_B C_2 = -D_A n_A \frac{\partial C_1}{\partial x} + V_A n_A C_1 \text{ when } \quad x = L_1 \tag{8}$$

$$-D_B n_B \frac{\partial C_2}{\partial x} + V_B n_B C_2 = -D_A n_A \frac{\partial C_3}{\partial x} + V_A n_A C_3 \text{ when } \quad x = L_A + L_B \tag{9}$$

$$q_A = q_B \Rightarrow V_A n_A = V_B n_B \Rightarrow V_B = V_A \frac{n_A}{n_B} \tag{10}$$

SOLUTION I

$0 \le x \le L_A$: $$D_A \frac{\partial^2 C_1}{\partial x^2} - V_A \frac{\partial C_1}{\partial x} - \lambda_A C_1 = 0 \qquad (1)$$

The characteristic equation is:

$$D_A x^2 - V_A x - \lambda_A = 0$$
$$\Delta_A = V_A^2 + 4\lambda_A D_A > 0$$

a_1 and a_2 are the solutions to the equation above:

$$a_1 = \frac{V_A - \sqrt{\Delta_A}}{2D_A} = \frac{V_A - \sqrt{V_A^2 + 4\lambda_A D_A}}{2D_A} < 0$$
$$a_2 = \frac{V_A + \sqrt{\Delta_A}}{2D_A} = \frac{V_A + \sqrt{V_A^2 + 4\lambda_A D_A}}{2D_A} > 0$$

$$0 \le x \le L_A \qquad C_1(x) = Ae^{a_1 x} + Be^{a_2 x}$$

A and B are coefficients to be determined later using the boundary conditions.

$L_A \le x \le L_A + L_B$: $$D_B \frac{\partial^2 C_2}{\partial x^2} - V_B \frac{\partial C_2}{\partial x} - \lambda_B C_2 = 0 \qquad (2)$$

The characteristic equation is:

$$D_B x^2 - V_B x - \lambda_B = 0$$
$$\Delta_B = V_B^2 + 4\lambda_B D_B > 0$$

b_1 and b_2 are the solutions to the equation above:

$$b_1 = \frac{V_B - \sqrt{\Delta_B}}{2D_B} = \frac{V_B - \sqrt{V_B^2 + 4\lambda_B D_B}}{2D_B} < 0$$
$$b_2 = \frac{V_B + \sqrt{\Delta_B}}{2D_B} = \frac{V_B + \sqrt{V_B^2 + 4\lambda_B D_B}}{2D_B} > 0$$

$$L_A \le x \le L_A + L_B \qquad C_2(x) = Ee^{b_1 x} + Fe^{b_2 x}$$

E and F are coefficients to be determined later using the boundary conditions.

$$x \ge L_A + L_B: \qquad D_A \frac{\partial^2 C_3}{\partial x^2} - V_A \frac{\partial C_3}{\partial x} - \lambda_A C_3 = 0 \tag{3}$$

The characteristic equation is:

$$D_A x^2 - V_A x - \lambda_A = 0$$
$$\Delta_A = V_A^2 + 4\lambda_A D_A > 0$$

a_1 and a_2 are the solutions to the equation above:

$$a_1 = \frac{V_A - \sqrt{\Delta_A}}{2D_A} = \frac{V_A - \sqrt{V_A^2 + 4\lambda_A D_A}}{2D_A} < 0$$
$$a_2 = \frac{V_A + \sqrt{\Delta_A}}{2D_A} = \frac{V_A + \sqrt{V_A^2 + 4\lambda_A D_A}}{2D_A} > 0$$

$$x \ge L_A + L_B \qquad C_3(x) = Ge^{a_1 x} + He^{a_2 x}$$

G and H are coefficients to be determined later using the boundary conditions.

Using Boundary conditions

- $C_1(x=0) = C_s$ (4)

Using $0 \le x \le L_A$ $C_1(x) = Ae^{a_1 x} + Be^{a_2 x}$

$$C_1(x=0) = Ae^{a_1 * 0} + Be^{a_2 * 0} = C_s \Rightarrow A + B = C_s \quad (I)$$

- $C_3(x) \xrightarrow{x \longrightarrow +\infty} 0$ (5)

Using $x \ge L_A + L_B$ $C_3(x) = Ge^{a1x} + He^{a2x}$ where :

$$a_1 = \frac{V_A - \sqrt{\Delta_A}}{2D_A} = \frac{V_A - \sqrt{V_A^2 + 4\lambda_A D_A}}{2D_A} < 0$$

$$a_2 = \frac{V_A + \sqrt{\Delta_A}}{2D_A} = \frac{V_A + \sqrt{V_A^2 + 4\lambda_A D_A}}{2D_A} > 0$$

So,

$$C_3(x) = Ge^{a1x} + He^{a2x} \xrightarrow{x \longrightarrow +\infty} 0 \text{ only if } H = 0$$

- $C_1(x = L_A) = C_2(x = L_A)$ (6)

Using: $0 \le x \le L_A$ $C_1(x) = Ae^{a_1 x} + Be^{a_2 x}$

and

$L_A \le x \le L_A + L_B$ $C_2(x) = Ee^{b_1 x} + Fe^{b_2 x}$

$$Ae^{a_1 L_A} + Be^{a_2 L_A} = Ee^{b_1 L_A} + Fe^{b_2 L_A}$$

$$\Rightarrow \quad Ae^{a_1 L_A} + Be^{a_2 L_A} - Ee^{b_1 L_A} - Fe^{b_2 L_A} = 0 \qquad (II)$$

- $C_2(x = L_A + L_B) = C_3(x = L_A + L_B)$ (7)

Using $L_A \le x \le L_A + L_B$ $\qquad C_2(x) = Ee^{b_1 x} + Fe^{b_2 x}$

and

$x \ge L_A + L_B$ $\qquad C_3(x) = Ge^{a_1 x}$

$$Ee^{b_1 (L_A + L_B)} + Fe^{b_2 (L_A + L_B)} = Ge^{a_1 (L_A + L_B)}$$

$$\Rightarrow \quad Ee^{b_1 (L_A + L_B)} + Fe^{b_2 (L_A + L_B)} - Ge^{a_1 (L_A + L_B)} = 0 \qquad (III)$$

- $-D_B n_B \frac{\partial C_2}{\partial x} + V_B n_B C_2 = -D_A n_A \frac{\partial C_1}{\partial x} + V_A n_A C_1$ when $x = L_A$ (8)

Using $0 \le x \le L_A$ $\qquad C_1(x) = Ae^{a_1 x} + Be^{a_2 x}$

and

$L_A \le x \le L_A + L_B$ $\qquad C_2(x) = Ee^{b_1 x} + Fe^{b_2 x}$

So,

$$\frac{\partial C_1}{\partial x}(x) = Aa_1 e^{a_1 x} + Ba_2 e^{a_2 x}$$

$$\frac{\partial C_2}{\partial x}(x) = Eb_1 e^{b_1 x} + Fb_2 e^{b_2 x}$$

$$-D_B n_B \frac{\partial C_2}{\partial x} + V_B n_B C_2 = -D_A n_A \frac{\partial C_1}{\partial x} + V_A n_A C_1$$

$\Leftrightarrow$

$$-D_B n_B (Eb_1 e^{b_1 L_A} + Fb_2 e^{b_2 L_A}) + V_B n_B (Ee^{b_1 L_A} + Fe^{b_2 L_A}) = -D_A n_A (Aa_1 e^{a_1 L_A} + Ba_2 e^{a_2 L_A}) +$$

$$V_A n_A (Ae^{a_1 L_A} + Be^{a_2 L_A})$$

$\Leftrightarrow$

$$Ae^{a_1 L_A}(-D_A n_A a_1 + V_A n_A) + Be^{a_2 L_A}(V_A n_A - D_A n_A a_2) - Ee^{b_1 L_A}(-D_B n_B b_1 + V_B n_B)$$
$$- Fe^{b_2 L_A}(V_B n_B - D_B n_B b_2) = 0$$

$$(IV)$$

- $-D_B n_B \frac{\partial C_2}{\partial x} + V_B n_B C_2 = -D_A n_A \frac{\partial C_3}{\partial x} + V_A n_A C_3$ when $x = L_A + L_B$ (9)

Using $L_A \le x \le L_A + L_B$ $C_2(x) = Ee^{b_1 x} + Fe^{b_2 x}$

and

$x \ge L_A + L_B$ $C_3(x) = Ge^{a_1 x}$

$$-D_B n_B (Eb_1 e^{b_1(L_A+L_B)} + Fb_2 e^{b_2(L_A+L_B)}) + V_B n_B (Ee^{b_1(L_A+L_B)} + Fe^{b_2(L_A+L_B)}) =$$
$$-D_A n_A G a_1 e^{a_1(L_A+L_B)} + V_A n_A G e^{a_1(L_A+L_B)}$$

So,

$$Ee^{b_1(L_A+L_B)}(-D_B n_B b_1 + V_B n_B) + Fe^{b_2(L_A+L_B)}(V_B n_B - D_B n_B b_2)$$
$$-Ge^{a_1(L_A+L_B)}(-D_A n_A a_1 + V_A n_A) = 0$$
$$(V)$$

Equations (I) to (V) constitute a system of 5 variables A, B, E, F and G. Solving this system will determine the 5 unknown variables.

$$\left\{\begin{array}{r} A+B=C_s \quad (I) \\ Ae^{a_1L_A}+Be^{a_2L_A}-Ee^{b_1L_A}-Fe^{b_2L_A}=0 \quad (II) \\ Ee^{b_1(L_A+L_B)}+Fe^{b_2(L_A+L_B)}-Ge^{a_1(L_A+L_B)}=0 \quad (III) \\ Ae^{a_1L_A}(-D_An_Aa_1+V_An_A)+Be^{a_2L_A}(V_An_A-D_An_Aa_2)- \\ Ee^{b_1L_A}(-D_Bn_Bb_1+V_Bn_B)-Fe^{b_2L_A}(V_Bn_B-D_Bn_Bb_2)=0 \quad (IV) \\ Ee^{b_1(L_A+L_B)}(-D_Bn_Bb_1+V_Bn_B)+Fe^{b_2(L_A+L_B)}(V_Bn_B-D_Bn_Bb_2) \\ -Ge^{a_1(L_A+L_B)}(-D_An_Aa_1+V_An_A)=0 \quad (V) \end{array}\right\}$$

This system is written as $M*V=V_0$ where $V=\begin{pmatrix} A \\ B \\ E \\ F \\ G \end{pmatrix}$ and $V_0=\begin{pmatrix} C_s \\ 0 \\ 0 \\ 0 \\ 0 \end{pmatrix}$ where M is:

$$\begin{bmatrix} 1 & 1 & 0 & 0 & 0 \\ e^{a_1L_A} & e^{a_2L_A} & -e^{b_1L_A} & -e^{b_2L_A} & 0 \\ 0 & 0 & e^{b_1(L_A+L_B)} & e^{b_2(L_A+L_B)} & -e^{a_1(L_A+L_B)} \\ e^{a_1L_A}(-D_An_Aa_1+V_An_A) & e^{a_2L_A}(-D_An_Aa_2+V_An_A) & -e^{b_1L_A}(-D_Bn_Bb_1+V_Bn_B) & -e^{b_2L_A}(-D_Bn_Bb_2+V_Bn_B) & 0 \\ 0 & 0 & e^{b_1(L_A+L_B)}(-D_Bn_Bb_1+V_Bn_B) & e^{b_2(L_A+L_B)}(-D_Bn_Bb_2+V_Bn_B) & -e^{a_1(L_A+L_B)}(-D_An_Aa_1+V_An_A) \end{bmatrix}$$

Solving the system of equations:

(III): $Ee^{b_1(L_A+L_B)} + Fe^{b_2(L_A+L_B)} - Ge^{a_1(L_A+L_B)} = 0$

By multiplying (III) with $(-D_A n_A a_1 + V_A n_A)$ the equation becomes:

$$Ee^{b1(LA+LB)}(-D_A n_A a_1 + V_A n_A) + Fe^{b2(LA+LB)}(-D_A n_A a_1 + V_A n_A) - Ge^{a1(LA+LB)}(-D_A n_A a_1 + V_A n_A) = 0 \quad (III)$$

And since equation (V) is:

$$Ee^{b1(LA+LB)}(-D_B n_B b_1 + V_B n_B) + Fe^{b2(LA+LB)}(V_B n_B - D_B n_B b_2) - Ge^{a1(LA+LB)}(-D_A n_A a_1 + V_A n_A) = 0 \quad (V)$$

The difference between the equations (III') and (V) gives:

$$Ee^{b1(LA+LB)}(-D_A n_A a_1 + V_A n_A) + Fe^{b2(LA+LB)}(-D_A n_A a_1 + V_A n_A) - Ge^{a1(LA+LB)}(-D_A n_A a_1 + V_A n_A)$$
$$-Ee^{b1(LA+LB)}(-D_B n_B b_1 + V_B n_B) - Fe^{b2(LA+LB)}(V_B n_B - D_B n_B b_2) + Ge^{a1(LA+LB)}(-D_A n_A a_1 + V_A n_A) = 0$$

$\Leftrightarrow$

$$Ee^{b1(LA+LB)}(-D_A n_A a_1 + V_A n_A) + Fe^{b2(LA+LB)}(-D_A n_A a_1 + V_A n_A) - Ee^{b1(LA+LB)}(-D_B n_B b_1 + V_B n_B) -$$
$$Fe^{b2(LA+LB)}(V_B n_B - D_B n_B b_2) = 0$$

$\Leftrightarrow$

$$Ee^{b1(LA+LB)}(D_A n_A a_1 - V_A n_A - D_B n_B b_1 + V_B n_B) + Fe^{b2(LA+LB)}(D_A n_A a_1 - V_A n_A + V_B n_B - D_B n_B b_2) = 0$$

$$\Leftrightarrow F = -E\frac{e^{b1(LA+LB)}(D_A n_A a_1 - V_A n_A - D_B n_B b_1 + V_B n_B)}{e^{b2(LA+LB)}(D_A n_A a_1 - V_A n_A + V_B n_B - D_B n_B b_2)}$$

$$\Leftrightarrow F = -Ee^{(b1-b2)*(LA+LB)}\frac{D_A n_A a_1 - V_A n_A - D_B n_B b_1 + V_B n_B}{D_A n_A a_1 - V_A n_A + V_B n_B - D_B n_B b_2}$$

$$\Leftrightarrow F = C_1 E \text{ with } C_1 = \left(\frac{D_A n_A a_1 - V_A n_A - D_B n_B b_1 + V_B n_B}{D_A n_A a_1 - V_A n_A - D_B n_B b_2 + V_B n_B}\right) * e^{(b_1-b_2)(L_A+L_B)}$$

Using the result above equation (II) becomes:

$$\text{(II): } Ae^{a1*LA} + Be^{a2*LA} - Ee^{b1*LA} - Fe^{b2*LA} = 0$$
$$\Leftrightarrow Ae^{a1*LA} + Be^{a2*LA} - Ee^{b1*LA} - C_1 Ee^{b2*LA} = 0$$
$$\Leftrightarrow Ae^{a1*LA} + Be^{a2*LA} - E(e^{b1*LA} + C_1 e^{b2*LA}) = 0$$
$$(II')$$

(IV):

$$Ae^{a1*LA}(-D_A n_A a_1 + V_A n_A) + Be^{a2*LA}(V_A n_A - D_A n_A a_2) - Ee^{b1*LA}(-D_B n_B b_1 + V_B n_B) - Fe^{b2*LA}(V_B n_B - D_B n_B b_2) = 0$$
$$\Leftrightarrow$$
$$Ae^{a1*LA}(-D_A n_A a_1 + V_A n_A) + Be^{a2*LA}(V_A n_A - D_A n_A a_2) - E(e^{b1*LA}(-D_B n_B b_1 + V_B n_B) + C_1 e^{b2*LA}(V_B n_B - D_B n_B b_2)) = 0$$
$$(IV)$$

Using equations (II') and (IV') such as :

(II')* $(e^{b1*LA}(-D_B n_B b_1 + V_B n_B) + C_1 e^{b2*LA}(V_B n_B - D_B n_B b_2))$ -(IV')* $(e^{b1*LA} + C_1 e^{b2*LA})$ to eliminate E from the equation:

$$(e^{b1*LA}(-D_B n_B b_1 + V_B n_B) + C_1 e^{b2*LA}(V_B n_B - D_B n_B b_2)) * (Ae^{a1*LA} + Be^{a2*LA} - E(e^{b1*LA} + C_1 e^{b2*LA})) -$$
$$(Ae^{a1*LA}(-D_A n_A a_1 + V_A n_A) + Be^{a2*LA}(V_A n_A - D_A n_A a_2) - E(e^{b1*LA}(-D_B n_B b_1 + V_B n_B) + \quad \Leftrightarrow$$
$$C_1 e^{b2*LA}(V_B n_B - D_B n_B b_2))) * (e^{b1*LA} + C_1 e^{b2*LA}) = 0$$
$$(e^{b1*LA}(-D_B n_B b_1 + V_B n_B) + C_1 e^{b2*LA}(V_B n_B - D_B n_B b_2)) * (Ae^{a1*LA} + Be^{a2*LA}) - (Ae^{a1*LA}(-D_A n_A a_1 + V_A n_A) + \quad \Leftrightarrow$$
$$Be^{a2*LA}(V_A n_A - D_A n_A a_2) + C_1 e^{b2*LA}(V_B n_B - D_B n_B b_2))) * (e^{b1*LA} + C_1 e^{b2*LA}) = 0$$
$$A(e^{(a1+b1)*LA}(D_B n_B b_1 - D_A n_A a_1) + C_1 e^{(a1+b2)*LA}(-D_A n_A a_1 + D_B n_B b_2)) + B(e^{(a2+b1)*LA}(D_B n_B b_1 - D_A n_A a_2) +$$
$$C_1 e^{(a2+b2)*LA}(-D_A n_A a_2 + D_B n_B b_2)) = 0$$

Dividing by $D_B n_B$ and since equation (I) gives $B = C_s - A$ the equation becomes:

$$A(e^{(a1+b1)*LA}(b_1 - A_2 a_1) + C_1 e^{(a1+b2)*LA}(b_2 - A_2 a_1)) + (C_s - A) * (e^{(a2+b1)*LA}(b_1 - A_2 a_2) +$$
$$C_1 e^{(a2+b2)*LA}(b_2 - A_2 a_2)) = 0$$
$$\text{where} \qquad A_2 = \frac{D_A n_A}{D_B n_B}$$

$$\Leftrightarrow$$

$$A(e^{(a1+b1)*LA}(b_1-A_2a_1)+C_1e^{(a1+b2)*LA}(b_2-A_2a_1)-(e^{(a2+b1)*LA}(b_1-A_2a_2)+C_1e^{(a2+b2)*LA}(b_2-A_2a_2))=$$

$$-C_s*(e^{(a2+b1)*LA}(b_1-A_2a_2)+C_1e^{(a2+b2)*LA}(b_2-A_2a_2)) \Leftrightarrow$$

$$A=-C_s*\frac{(e^{(a2+b1)*LA}(b_1-A_2a_2)+C_1e^{(a2+b2)*LA}(b_2-A_2a_2))}{(e^{(a1+b1)*LA}(b_1-A_2a_1)+C_1e^{(a1+b2)*LA}(b_2-A_2a_1)-(e^{(a2+b1)*LA}(b_1-A_2a_2)+C_1e^{(a2+b2)*LA}(b_2-A_2a_2))}$$

$$\Leftrightarrow$$

$$A=-C_s*\frac{(e^{(a2+b1)*LA}(b_1-A_2a_2)+C_1e^{(a2+b2)*LA}(b_2-A_2a_2))}{(e^{(a1+b1)*LA}(b_1-A_2a_1)+C_1e^{(a1+b2)*LA}(b_2-A_2a_1)-(e^{(a2+b1)*LA}(b_1-A_2a_2)+C_1e^{(a2+b2)*LA}(b_2-A_2a_2))}$$

$$A=-C_s*\frac{1}{1-\frac{(e^{(a1+b1)*LA}(b_1-A_2a_1)+C_1e^{(a1+b2)*LA}(b_2-A_2a_1)}{(e^{(a2+b1)*LA}(b_1-A_2a_2)+C_1e^{(a2+b2)*LA}(b_2-A_2a_2))}}$$

$$A=C_sC_2 \text{ with } C_2=-\frac{1}{1-\frac{(e^{(a1+b1)*LA}(b_1-A_2a_1)+C_1e^{(a1+b2)*LA}(b_2-A_2a_1)}{(e^{(a2+b1)*LA}(b_1-A_2a_2)+C_1e^{(a2+b2)*LA}(b_2-A_2a_2))}}$$

$$C_2=\frac{1}{C_2'-1}$$

$$C_2'=\left(\frac{e^{(a_1+b_1)L_A}(b_1-A_2a_1)+C_1e^{(a_1+b_2)L_A}(b_2-A_2a_1)}{e^{(a_2+b_1)L_A}(b_1-A_2a_2)+C_1e^{(a_2+b_2)L_A}(b_2-A_2a_2)}\right)$$

(II): $Ae^{a1*LA}+Be^{a2*LA}-Ee^{b1*LA}-Fe^{b2*LA}=0$

$$C_s*C_2e^{a1*LA}+(1-C_2)*C_se^{a2*LA}-Ee^{b1*LA}-C_1Ee^{b2*LA}=0$$

$$\Leftrightarrow$$

$$E=C_s\frac{C_2e^{a1*LA}+(1-C_2)e^{a2*LA}}{e^{b1*LA}+C_1e^{b2*LA}}$$

$$E=C_sC_3 \text{ with } C_3=\frac{C_2e^{a_1L_A}+(1-C_2)e^{a_2L_A}}{e^{b_1L_A}+C_1e^{b_2L_A}}$$

$$F = C_s C_1 C_3$$

(III): $Ee^{b1(LA+LB)} + Fe^{b2(LA+LB)} - Ge^{a1(LA+LB)} = 0$

$$\Leftrightarrow G = \frac{Ee^{b_1(L_A+L_B)} + Fe^{b_2(L_A+L_B)}}{e^{a_1(L_A+L_B)}}$$

$$\Leftrightarrow G = C_s C_3 \frac{e^{b_1(L_A+L_B)} + C_1 e^{b_2(L_A+L_B)}}{e^{a_1(L_A+L_B)}}$$

$$\Leftrightarrow G = C_s C_4 \text{ where } C_4 = C_3 \frac{e^{b_1(L_A+L_B)} + C_1 e^{b_2(L_A+L_B)}}{e^{a_1(L_A+L_B)}}$$

Summary of solutions:

$$0 \le x \le L_A \qquad \frac{C_1(x)}{C_s} = C_2 e^{a_1 x} + (1 - C_2) e^{a_2 x}$$

$$L_A \le x \le L_A + L_B \qquad \frac{C_2(x)}{C_s} = C_3 (e^{b_1 x} + C_1 e^{b_2 x})$$

$$x \ge L_A + L_B \qquad \frac{C_3(x)}{C_s} = C_4 e^{a1 x}$$

Where

$$\mathrm{C}_1 = \left(\frac{D_A n_A a_1 - V_A n_A - D_B n_B b_1 + V_B n_B}{D_A n_A a_1 - V_A n_A - D_B n_B b_2 + V_B n_B} \right) * e^{(b_1 - b_2)(L_A + L_B)}$$

$$C_2 = \frac{1}{C_2' - 1} \quad \textit{and} \quad C_2' = \left(\frac{e^{(a_1+b_1)L_A}(b_1 - A_2 a_1) + C_1 e^{(a_1+b_2)L_A}(b_2 - A_2 a_1)}{e^{(a_2+b_1)L_A}(b_1 - A_2 a_2) + C_1 e^{(a_2+b_2)L_A}(b_2 - A_2 a_2)} \right)$$

$$A_2 = \frac{D_A n_A}{D_B n_B}$$

$$C_3 = \frac{C_2 e^{a_1 L_A} + (1 - C_2) e^{a_2 L_A}}{e^{b_1 L_A} + C_1 e^{b_2 L_A}}$$

$$C_4 = C_3 \frac{e^{b_1 (L_A + L_B)} + C_1 e^{b_2 (L_A + L_B)}}{e^{a_1 (L_A + L_B)}}$$

$$C_1 = \left(\frac{D_A n_A a_1 - V_A n_A - D_B n_B b_1 + V_B n_B}{D_A n_A a_1 - V_A n_A - D_B n_B b_2 + V_B n_B} \right) * e^{(b_1 - b_2)(L_A + L_B)}$$

Division by $D_A n_A a_1 - V_A n_A \Rightarrow$

$$C_1 = \left(\frac{1 - \frac{D_B n_B b_1 - V_B n_B}{D_A n_A a_1 - V_A n_A}}{1 - \frac{D_B n_B b_2 - V_B n_B}{D_A n_A a_1 - V_A n_A}} \right) * e^{(b_1 - b_2)(L_A + L_B)}$$

Division by $V_A n_A \Rightarrow$

$$C_1 = \left(\frac{1 - \frac{\frac{D_B n_B b_1}{V_A n_A} - \frac{V_B n_B}{V_A n_A}}{\frac{D_A n_A a_1}{V_A n_A} - 1}}{1 - \frac{\frac{D_B n_B b_2}{V_A n_A} - \frac{V_B n_B}{V_A n_A}}{\frac{D_A n_A a_1}{V_A n_A} - 1}} \right) * e^{(b_1 - b_2)(L_A + L_B)}$$

Since the flow going in the PRB equals the flow going out: $\frac{V_B n_B}{V_A n_A} = 1$

So, $\frac{D_B n_B b_1}{V_A n_A} = \frac{D_B b_1}{V_B} = \frac{b_1 L_B}{L_B V_B / D_B} = \frac{NAC_B}{P_e^B}$,

$\frac{D_B n_B b_2}{V_A n_A} = \frac{D_B b_2}{V_B} = \frac{b_2 L_B}{L_B V_B / D_B} = \frac{\overline{NAC_B}}{P_e^B}$,

and $\frac{D_A n_A a_1}{V_A n_A} = \frac{a_1 L_A}{L_A V_A / D_A} = \frac{NAC_A}{P_e^A}$

$$C_1 = \left(\frac{1 - \frac{\frac{NAC_B}{P_e^B} - 1}{\frac{NAC_A}{P_e^A} - 1}}{1 - \frac{\frac{\overline{NAC_B}}{P_e^B} - 1}{\frac{\overline{NAC_A}}{P_e^A} - 1}} \right) * e^{(b_1 - b_2)(L_A + L_B)}$$

By definition $NAC_A = \frac{1}{2}\left[P_e^A - \sqrt{(P_e^A)^2 + 4Dk_A P_e^A}\right]$, $NAC_B = \frac{1}{2}\left[P_e^B - \sqrt{(P_e^B)^2 + 4Dk_B P_e^B}\right]$

and its respective conjugates:

$\overline{NAC_A} = \frac{1}{2}\left[P_e^A + \sqrt{(P_e^A)^2 + 4Dk_A P_e^A}\right]$, $\overline{NAC_B} = \frac{1}{2}\left[P_e^B + \sqrt{(P_e^B)^2 + 4Dk_B P_e^B}\right]$

Knowing:

$$a_1 = \frac{V_A - \sqrt{V_A^2 + 4\lambda_A D_A}}{2D_A} \qquad a_2 = \frac{V_A + \sqrt{V_A^2 + 4\lambda_A D_A}}{2D_A}$$

$$b_1 = \frac{V_B - \sqrt{V_B^2 + 4\lambda_B D_B}}{2D_B} \qquad b_2 = \frac{V_B + \sqrt{V_B^2 + 4\lambda_B D_B}}{2D_B}$$

We can verify that:

$$a_1 L_A = NAC_A \qquad a_2 L_A = \overline{NAC_A}$$

$$b_1 L_B = NAC_B \qquad b_2 L_B = \overline{NAC_B}$$

Let's define δ_A, $\overline{\delta_A}$, δ_B and $\overline{\delta_B}$ as follows:

$$\delta_A = \frac{1}{2}\left(1-\sqrt{1+4\frac{Dk_A}{P_e^A}}\right) \text{ and its conjugate } \quad \overline{\delta_A} = \frac{1}{2}\left(1+\sqrt{1+4\frac{Dk_A}{P_e^A}}\right)$$

$$\delta_B = \frac{1}{2}\left(1-\sqrt{1+4\frac{Dk_B}{P_e^B}}\right) \text{ and its conjugate } \quad \overline{\delta_B} = \frac{1}{2}\left(1+\sqrt{1+4\frac{Dk_B}{P_e^B}}\right)$$

So,

$$\frac{NAC_A}{P_e^A} = \delta_A \ , \ \frac{NAC_B}{P_e^B} = \delta_B \ ,$$
$$\frac{\overline{NAC_A}}{P_e^A} = \overline{\delta_A} \text{ and } \frac{\overline{NAC_B}}{P_e^B} = \overline{\delta_B}$$

$$C_1 = \left(\frac{1-\dfrac{\delta_B - 1}{\delta_A - 1}}{1-\dfrac{\overline{\delta_B} - 1}{\delta_A - 1}}\right) * e^{(b_1-b_2)(L_A+L_B)}$$

$$C_1 = \left(\frac{\delta_A - \delta_B}{\delta_A - \overline{\delta_B}}\right) * e^{(b_1-b_2)(L_A+L_B)}$$

And since

$$(b_1-b_2)(L_A+L_B) = (b_1L_B - b_2L_B)(1+L_A/L_B) = (NAC_B - \overline{NAC_B})(1+1/L_B^R)$$
$$= -(1+1/L_B^R)\sqrt{P_e^{B^2}+4Dk_BP_e^B}$$

with $\quad L_B^R = \dfrac{L_B}{L_A}$

Let's define the function Ψ so that $\Psi(X_1, X_2, X_3, X_4) = \dfrac{X_1 - X_2}{X_3 - X_4}$

$$C_1 = Q_1^* \exp\left(-(1+1/L_B^R)\sqrt{P_e^{B^2}+4Dk_BP_e^B}\right) \quad \text{where} \quad Q_1^* = \Psi(\delta_A, \delta_B, \delta_A, \overline{\delta_B})$$

$$C_2 = \frac{1}{C_2' - 1}$$

$$C_2' = \left(\frac{e^{(a_1+b_1)L_A}(b_1 - A_2 a_1) + C_1 e^{(a_1+b_2)L_A}(b_2 - A_2 a_1)}{e^{(a_2+b_1)L_A}(b_1 - A_2 a_2) + C_1 e^{(a_2+b_2)L_A}(b_2 - A_2 a_2)} \right)$$

Division by $e^{(a_1+b_1)L_A}(b_1 - A_2 a_1)$

$$C_2' = \frac{1 + C_1 e^{(b_2-b_1)L_A} * \dfrac{b_2 - A_2 a_1}{b_1 - A_2 a_1}}{e^{(a_2-a_1)L_A}\left(\dfrac{b_1 - A_2 a_2}{b_1 - A_2 a_1} + C_1 e^{(b_2-b_1)L_A} * \dfrac{b_2 - A_2 a_2}{b_1 - A_2 a_1} \right)}$$

With $A_2 = \dfrac{D_A n_A}{D_B n_B}$

and since $P_e^A = \dfrac{L_A v_A}{D_A}$ and $P_e^B = \dfrac{L_B v_B}{D_B}$ then $\dfrac{P_e^A}{P_e^B} = \dfrac{L_A v_A}{D_A} * \dfrac{D_B}{L_B v_B} = \dfrac{L_A}{L_B} * \dfrac{1}{A_2}$ then $A_2 = \dfrac{L_A P_e^B}{L_B P_e^A}$

$$\frac{b_2 - A_2 a_1}{b_1 - A_2 a_1} = \frac{\dfrac{b_2}{A_2 a_1} - 1}{\dfrac{b_1}{A_2 a_1} - 1} = \frac{\dfrac{\overline{NAC_B}}{NAC_A} * \dfrac{P_e^A}{P_e^B} - 1}{\dfrac{NAC_B}{NAC_A} * \dfrac{P_e^A}{P_e^B} - 1} = \frac{\overline{NAC_B} * P_e^A - NAC_A * P_e^B}{NAC_B * P_e^A - NAC_A * P_e^B} = \frac{\dfrac{\overline{NAC_B}}{P_e^B} - \dfrac{NAC_A}{P_e^A}}{\dfrac{NAC_B}{P_e^B} - \dfrac{NAC_A}{P_e^A}} = \frac{\overline{\delta_B} - \delta_A}{\delta_B - \delta_A}$$

because $\dfrac{b_2}{A_2 a_1} = \dfrac{b_2 L_B P_e^A}{a_1 L_A P_e^B} = \dfrac{\overline{NAC_B}}{NAC_A} * \dfrac{P_e^A}{P_e^B}$ and $\dfrac{b_1}{A_2 a_1} = \dfrac{b_1 L_B P_e^A}{a_1 L_A P_e^B} = \dfrac{NAC_B}{NAC_A} * \dfrac{P_e^A}{P_e^B}$

And,

$$\frac{b_1 - A_2 a_2}{b_1 - A_2 a_1} = \frac{\dfrac{b_1}{A_2 a_2} - 1}{\dfrac{b_1}{A_2 a_2} - \dfrac{a_1}{a_2}} = \frac{\dfrac{NAC_B}{\overline{NAC_A}} * \dfrac{P_e^A}{P_e^B} - 1}{\dfrac{NAC_B}{\overline{NAC_A}} * \dfrac{P_e^A}{P_e^B} - \dfrac{NAC_A}{\overline{NAC_A}}} = \frac{NAC_B * P_e^A - \overline{NAC_A} * P_e^B}{NAC_B * P_e^A - NAC_A * P_e^B} = \frac{\dfrac{NAC_B}{P_e^B} - \dfrac{\overline{NAC_A}}{P_e^A}}{\dfrac{NAC_B}{P_e^B} - \dfrac{NAC_A}{P_e^A}} = \frac{\delta_B - \overline{\delta_A}}{\delta_B - \delta_A}$$

Because $\dfrac{b_1}{A_2 a_2} = \dfrac{b_1 L_B P_e^A}{a_2 L_A P_e^B} = \dfrac{NAC_B}{\overline{NAC_A}} * \dfrac{P_e^A}{P_e^B}$ and $\dfrac{a_1}{a_2} = \dfrac{a_1 L_A}{a_2 L_A} = \dfrac{NAC_A}{\overline{NAC_A}}$

And,

$$\frac{b_2 - A_2 a_2}{b_1 - A_2 a_1} = \frac{\frac{b_2}{A_2 a_2} - 1}{\frac{b_1}{A_2 a_2} - \frac{a_1}{a_2}} = \frac{\frac{\overline{NAC_B}}{\overline{NAC_A}} * \frac{P_e^A}{P_e^B} - 1}{\frac{NAC_B}{\overline{NAC_A}} * \frac{P_e^A}{P_e^B} - \frac{NAC_A}{\overline{NAC_A}}} = \frac{\overline{NAC_B} * P_e^A - \overline{NAC_A} * P_e^B}{NAC_B * P_e^A - NAC_A * P_e^B} = \frac{\frac{\overline{NAC_B}}{P_e^B} - \frac{\overline{NAC_A}}{P_e^A}}{\frac{NAC_B}{P_e^B} - \frac{NAC_A}{P_e^A}} = -1$$

because $\frac{b_2}{A_2 a_2} = \frac{b_2 L_B P_e^A}{a_2 L_A P_e^B} = \frac{\overline{NAC_B}}{\overline{NAC_A}} * \frac{P_e^A}{P_e^B}$

$$C_2^{'} = \frac{1 + C_1 e^{(b_2 - b_1) L_A} * \left(\frac{\overline{\delta_B} - \delta_A}{\delta_B - \delta_A} \right)}{e^{(a_2 - a_1) LA} \left(\frac{\delta_B - \overline{\delta_A}}{\delta_B - \delta_A} - C_1 e^{(b_2 - b_1) L_A} \right)}$$

$$C_1 = \left(\frac{\delta_A - \delta_B}{\delta_A - \overline{\delta_B}} \right) * e^{(b_1 - b_2)(L_A + L_B)} \quad so \; C_1 e^{(b_2 - b_1) L_A} * \left(\frac{\overline{\delta_B} - \delta_A}{\delta_B - \delta_A} \right) = \left(\frac{\delta_A - \delta_B}{\delta_A - \overline{\delta_B}} \right) * e^{(b_1 - b_2) L_B} * \left(\frac{\overline{\delta_B} - \delta_A}{\delta_B - \delta_A} \right) = e^{(b_1 - b_2) L_B}$$

And

$$C_1 = \left(\frac{\delta_A - \delta_B}{\delta_A - \overline{\delta_B}} \right) * e^{(b_1 - b_2)(L_A + L_B)} \quad so \quad -C_1 e^{(b_2 - b_1) L_A} = -\left(\frac{\delta_A - \delta_B}{\delta_A - \overline{\delta_B}} \right) * e^{(b_1 - b_2) L_B} = \left(\frac{\delta_B - \delta_A}{\delta_B - \overline{\delta_A}} \right) * e^{(b_1 - b_2) L_B}$$

because $\delta_B - \overline{\delta_A} = -\left(\overline{\delta_B} - \delta_A \right)$

Therefore,

$$C_2^{'} = \frac{1 + e^{(b_1 - b_2) L_B}}{e^{(a_2 - a_1) L_A} \left(\frac{\delta_B - \overline{\delta_A}}{\delta_B - \delta_A} + \left(\frac{\delta_B - \delta_A}{\delta_B - \overline{\delta_A}} \right) * e^{(b_1 - b_2) L_B} \right)}$$

$$C_2^{'} = \frac{1+e^{(b_1-b_2)L_B}}{e^{(a_2-a_1)L_A}\left(Q_2^* + \frac{e^{(b_1-b_2)L_B}}{Q_2^*}\right)} \qquad \text{With} \quad Q_2^* = \Psi(\delta_B, \overline{\delta_A}, \delta_B, \delta_A)$$

$$C_2^{'} = \frac{1+\exp(-\sqrt{P_e^{B^2} + 4Dk_B P_e^B})}{\left(Q_2^* + \frac{\exp(-\sqrt{P_e^{B^2} + 4Dk_B P_e^B})}{Q_2^*}\right) * \exp(\sqrt{P_e^{A^2} + 4Dk_A P_e^A})}$$

Since $C_3 = \frac{C_2 e^{a_1 L_A} + (1-C_2)e^{a_2 L_A}}{e^{b_1 L_A} + C_1 e^{b_2 L_A}}$

So,

$$C_3 = \frac{C_2 \exp(NAC_A^{nd}) + (1-C_2)\exp(\overline{NAC}_A^{nd})}{\exp(NAC_B^{nd} / L_B^R) + C_1 \exp(\overline{NAC}_B^{nd} / L_B^R)}$$

And,

$$C_4 = C_3 \frac{e^{b_1(L_A+L_B)} + C_1 e^{b_2(L_A+L_B)}}{e^{a_1(L_A+L_B)}}$$

$$C_4 = C_3 \frac{\exp\left(NAC_B^{nd}(1+1/L_B^R)\right) + C_1 \exp\left(\overline{NAC_B^{nd}}(1+1/L_B^R)\right)}{\exp\left(NAC_A^{nd}(1+L_B^R)\right)}$$

Appendix B

Solution I using dimensionless parameters

Let's define three dimensionless distance variables as follows:

$$\mathrm{X}_U = \frac{x}{L_A} \; ; \; \mathrm{X}_D = \frac{x - L_A - L_B}{L_{POC} - L_A - L_B} \; ; \text{ and } \; \mathrm{X}_B = \frac{x - L_A}{L_B}$$

and

$$L_{POC}^R = \frac{L_{POC} - L_A - L_B}{L_A} \quad ; \quad L_B^R = \frac{L_B}{L_A}$$

$$0 \le X_U \le 1 \;\; C_A^R(X_U) = C_2 \exp(NAC_A^{nd} X_U) + (1 - C_2)\exp(\overline{NAC_A^{nd}} X_U)$$

$$0 \le X_B \le 1 \;\; C_B^R(X_B) = C_3 \left(\exp(NAC_B^{nd} / L_B^R)\exp(NAC_B^{nd} X_B) + C_1 \exp(\overline{NAC_B^{nd}} / L_B^R)\exp(\overline{NAC_B^{nd}} X_B)\right)$$

$$0 \le X_D \le 1 \;\; C_A^R(X_D) = C_4 \exp\left(NAC_A^{nd}(1 + L_B^R)\right)\exp\left(NAC_A^{nd} L_{POC}^R X_D\right)$$

Where

$$\mathrm{C}_1 = Q_1^* \exp\left(-(1 + 1/L_B^R)\sqrt{P_e^{B^2} + 4Dk_B P_e^B}\right)$$

$$C_2 = \frac{1}{C_2' - 1}$$

$$C_2^{'} = \frac{1 + \exp(-\sqrt{P_e^{B^2} + 4Dk_B P_e^B})}{\left(Q_2^* + \frac{\exp(-\sqrt{P_e^{B^2} + 4Dk_B P_e^B})}{Q_2^*} \right) * \exp(\sqrt{P_e^{A^2} + 4Dk_A P_e^A})}$$

$$C_3 = \frac{C_2 \exp(NAC_A^{nd}) + (1 - C_2) \exp(\overline{NAC}_A^{nd})}{\exp(NAC_B^{nd} / L_B^R) + C_1 \exp(\overline{NAC}_B^{nd} / L_B^R)}$$

$$C_4 = C_3 \frac{\exp\left(NAC_B^{nd}(1 + 1/L_B^R)\right) + C_1 \exp\left(\overline{NAC}_B^{nd}(1 + 1/L_B^R)\right)}{\exp\left(NAC_A^{nd}(1 + L_B^R)\right)}$$

With

Ψ a function such that $\Psi(X_1, X_2, X_3, X_4) = \frac{X_1 - X_2}{X_3 - X_4}$

$$Q_1^* = \Psi(\delta_A, \delta_B, \delta_A, \overline{\delta_B})$$

$$Q_2^* = \Psi(\delta_B, \overline{\delta_A}, \delta_B, \delta_A)$$

MODEL II

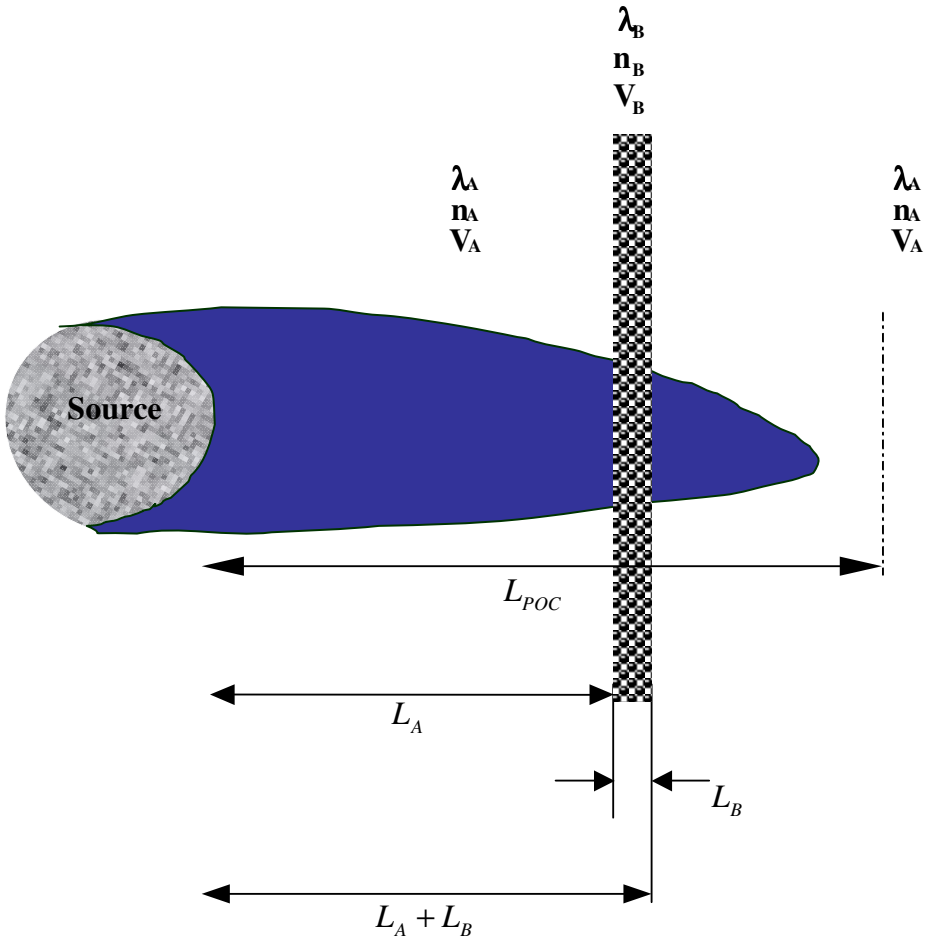

SOLUTION II

$0 \le x \le L_A$: $C_A(x) = C_s e^{-NAC_A * x}$

$L_A \le x \le L_A + L_B$: $C_B(x) = C_{B0} e^{-NAC_B * x}$

$L_A + L_B \le x \le L_{POC}$: $C_A(x) = C_{MCL} e^{-NAC_A * (x - L_{POC})}$

Where

$$NAC_A = \frac{-V_A + \sqrt{V_A^2 + 4D_A\lambda_A}}{2D_A}$$

and

$$NAC_B = \frac{-V_B + \sqrt{V_B^2 + 4D_B\lambda_B}}{2D_B}$$

Using the boundary conditions:

At $x = L_A$ $C_A(x = L_A) = C_s e^{-NAC_A * L_A} = C_{B0} e^{-NAC_B * L_A}$

$$C_{B0} = C_s e^{-(NAC_A - NAC_B)*L_A} \qquad \text{At } x = L_A + L_B$$

$$C_B(x = L_A + L_B) = C_{B0} e^{-NAC_B*(L_A+L_B)} = C_{MCL} e^{-NAC_A*(L_A+L_B-L_{POC})}$$

$$\Rightarrow C_s e^{-(NAC_A-NAC_B)*L_A} e^{-NAC_B*(L_A+L_B)} = C_{MCL} e^{-NAC_A*(L_A+L_B-L_{POC})}$$

$$\Rightarrow \frac{C_s}{C_{MCL}} = e^{NAC_A*L_A+NAC_B*L_B-NAC_A*(L_A+L_B-L_{POC})}$$

$$\Rightarrow \frac{C_s}{C_{MCL}} = e^{(NAC_B-NAC_A)*L_B+NAC_A*L_{POC}}$$

$$\Rightarrow$$

$$L_B = \frac{\ln\left(\frac{C_s}{C_{MCL}}\right) - NAC_A * L_{POC}}{NAC_B - NAC_A}$$

Solution II using dimensionless parameters

$$X_U = \frac{x}{L_A} \; ; \; X_D = \frac{x - L_A - L_B}{L_{POC} - L_A - L_B} \; ; \text{ and } \; X_B = \frac{x - L_A}{L_B}$$

and

$$L^R_{POC} = \frac{L_{POC} - L_A - L_B}{L_A} \quad ; \quad L^R_B = \frac{L_B}{L_A}$$

$0 \le x \le L_A$: $C_A(x) = C_s e^{-NAC_A * x}$ becomes:

$$0 \le X_U \le 1 \quad C^R_A(X_U) = \exp(-NAC^{nd}_A X_U)$$

$L_A \le x \le L_A + L_B$: $C_B(x) = C_{B0} e^{-NAC_B * x}$ With

$$C_{B0} = C_s e^{-(NAC_A - NAC_B) * L_A}$$

Since $X_B = \frac{x - L_A}{L_B} \Rightarrow x = X_B L_B + L_A$

$$0 \le X_B \le 1 \quad C^R_B(X_U) = \exp\left((-NAC_A + NAC_B)L_A\right) * \exp\left(-NAC_B(X_B L_B + L_A)\right)$$
$$= \exp(-NAC_A L_A) * \exp(-NAC_B X_B L_B)$$

So ,

$$0 \le X_B \le 1 \quad C^R_B(X_U) = \exp(-NAC^{nd}_A) * \exp(-NAC^{nd}_B X_B)$$

$L_A + L_B \le x \le L_{POC}$: $$C_A(x) = C_{MCL} e^{-NAC_A^*(x - L_{POC})}$$

$$X_D = \frac{x - L_A - L_B}{L_{POC} - L_A - L_B} \Rightarrow x = X_D(L_{POC} - L_A - L_B) + L_A + L_B$$

$$x - L_{POC} = (L_{POC} - L_A - L_B)(X_D - 1)$$

So,

$0 \le X_D \le 1 \quad C_A^R(X_D) = C_{MCL}^R \exp\left(-NAC_A(L_{POC} - L_A - L_B)(X_D - 1)\right)$

And since $L_{POC}^R = \frac{L_{POC} - L_A - L_B}{L_A}$

Therefore,

$$0 \le X_D \le 1 \quad C_A^R(X_D) = C_{MCL}^R \exp\left(-NAC_A^{nd} L_{POC}^R (X_D - 1)\right)$$